P-66

SUPERCONDUCTIVITY DEVICES: COMMERCIAL USE OF SPACE

Semi-Annual Report

to

National Aeronautics and Space Administration
Langley Research Center
Hampton, VA 23665-5225

Principal Investigator:
Gene Haertling

Supporting Investigators:
Chi-Shiung Hsi
LaDawn McIntyre
Guang Li

Contract No. NAG-1-1301

May 5, 1992

Department of Ceramic Engineering
College of Engineering
CLEMSON UNIVERSITY

SUPERCONDUCTIVITY DEVICES: COMMERCIAL USE OF SPACE

Semi-Annual Report

to

National Aeronautics and Space Administration
Langley Research Center
Hampton, VA 23665-5225

Principal Investigator:

Gene Haertling

Supporting Investigators:

Chi-Shiung Hsi
LaDawn McIntyre
Guang Li

Contract No. NAG-1-1301

May 5, 1992

CLEMSON
UNIVERSITY

Department of Ceramic Engineering
College of Engineering

I. Introduction

The high Tc (>95K) superconducting ceramic materials, initially developed in 1987, are now being extensively investigated for a variety of engineering applications. These applications include such devices as conducting links, rotating and linear bearings, sensors, filters, switches, high Q cavities, magnets and motors. Some of these devices take advantage of the material's ability to lose all electrical resistance at a critical temperature (Tc) while others make use of the repulsion forces generated between the magnetic field of a permanent magnet and a superconductor which is cooled below its Tc, i.e., the Meissner effect.

A device involving the first of these effects, i.e., loss of resistance at the onset of superconductivity, has been under development at Clemson University under the sponsorship of NASA Langley for the last three years. Known as a low thermal conductivity superconducting grounding link for the SAFIRE program, this device has undergone a full year of real time testing and has shown promise of meeting many of the original objectives.

A companion device to the grounding link in the SAFIRE application is the data link between the detectors and the preamps. In contrast to the former device which is a single conductor, the data link consists of a large number of electrically isolated leads of very small cross section which are designed to carry an electrical signal yet keep the thermal losses to a bare minimum. This application is obviously more demanding from a technical standpoint than the grounding link because the technologies involved in processing and fabricating small, multiple-leaded devices is considerably more complicated. Much of the work reported in this semi-annual report involves (1) the preparation and processing of the high temperature (>105K) 2223 Bi-Sr-Ca-Cu-O phase in relatively phase pure form, (2) the development of suitable substrate materials for the BSCCO, (3) screen printing of both the 123 $YBa_2Cu_3O_{7-x}$ and the 2223 BSCCO materials on the substrates and (4) evaluation of the resulting superconductors.

In addition to this device, development is also being carried out on the development of solid-state electromechanical actuators which can be used in a number of applications in space such as cryopumps motors, anti-vibration active structures and mirror correctors. Considering any of these applications, the key to the successful development of a device is the development of a ceramic material which will produce the maximum displacement per volt input. This is especially true of the cryocooler pump application where size, efficiency and reliability are of prime consideration. This report describes the work accomplished, to date, toward this goal; i.e., (1) a review of the present state of the art in actuator technology, (2) the fabrication and processing of high strain

electrostrictive materials and (3) the testing and evaluation of these electrostrictive materials.

The report is divided into three parts with Part I dealing with the processing and screen printing of the superconducting materials, Part II describing work on coprecipitation methods for achieving more single phase 2223 BSCCO materials and Part III reporting on the electromechanical actuator work.

Part I

Semi-Annual Report

SUPERCONDUCTIVITY DEVICES: COMMERCIAL USE OF SPACE

Screen Printed Y and Bi-Based Superconductors

to

National Aeronautics and Space Administration
Langley Research Center
Hampton, VA 23665-5225

Principal Investigator:
Gene H. Haertling -Clemson University

Supporting Investigator:
Chi-Shiung Hsi -Clemson University

Contract No: NAG-1-1301

April, 1992

Abstract

High T_c superconducting thick film were prepared by screen printing process. Y-based ($YBa_2Cu_3O_{7-x}$) superconducting thick films were printed on 211/ Al_2O_3, SNT/Al_2O_3, and YSZ substrates. Because of poor adhesion of the superconductor thick films to 211/ Al_2O_3 and SNT/Al_2O_3 substrates, relatively low T_c and J_c values were obtained from the films printed on these substrates. Critical temperatures (T_c) of $YBa_2Cu_3O_{7-x}$ thick films deposited on 211/ Al_2O_3 and SNT/Al_2O_3 substrates were about 80 K. The critical current densities (J_c) of these films were less than 2 A/cm^2. Higher T_c and J_c $YBa_2Cu_3O_{7-x}$ thick films were printed on YSZ substrates. A $YBa_2Cu_3O_{7-x}$ thick film with T_c=86.4 and J_c= 50.4 A/cm^2 was prepared by printing the film on YSZ substrate and firing at 990^{o}C for 10 minutes. Multiple-lead samples were also prepared on the YSZ substrates. The multiple-lead samples showed lower T_c and/ or J_c values than those of plain samples. The heat treatment conditions of the multiple-lead samples are still under investigation.

Bi-based superconductor thick films were printed on polycrystalline MgO substrates. Only low J_c BSCCO superconducting thick films have been obtained so far. Improving the superconducting properties of the BSCCO screen printed thick films will be emphasized in future work.

I. Introduction.

Among all the possible applications of high T_c superconductors, electric wiring, high information density data transmission lines, magnetic shielding, and hybrid technology will probably be the first high T_c components to be used. Sintering the high T_c superconductor with a large volume and area is necessary for these applications. Thick film technology, which can be applied under normal atmospheric conditions, is a promising method to achieve such components. Several thick film fabrication methods have recently been proposed and demonstrated, e.g., molten oxide process, rapid quench method, tape casting , spray pyrolysis, and screen printing.

A $YBa_2Cu_3O_{7-x}$ superconductor grounding link for an infrared detector on the SAFIRE program has been successfully developed by tape casting technology at Clemson University. In this application, the superconducting link provides a low noise, low thermal conductivity connection from the sensitive atmospheric detector at 4K and pre-amplifier at 80K. This serves to conserve the helium in space and will extend the life of mission. A companion device to the grounding link, in the SAFIRE program, is the data link between the detector and the pre-amplifier. The data link involves a large number of electrically isolated leads of very small cross section which are designed to reduce the thermal losses to a bare minimum. The screen print method as mentioned above is considered to be the most practical thick film process to fabricate the data link, because it is relatively simple, easy to pattern, and a low cost technique.

Films which were deposited by the screen printing process had numerous problems, the most serious of which was poor superconductivity. Since the properties of the copper oxide superconducting films are highly sensitive to the substrate materials[1]. Random orientation of the crystallities and poor interconnectivity were considered to be the reasons for the low values of T_c and J_c of the films. Since yttria-based ($YBa_2Cu_3O_{7-x}$) thick films have a more consistent fabrication process than those of the Bi-based or Tl-based materials, it was the first material used to develop and evaluate the multiple-lead devices. The Bi-

based and Tl-based superconductors are then to be developed and compared with the properties of the $YBa_2Cu_3O_{7-x}$ devices.

Currently, the $YBa_2Cu_3O_{7-x}$ superconductor screen printed thick films have been deposited on three kinds of substrate materials. In addition multiple-lead samples have been printed on YSZ (Yittrium Stabilized Zirconia) substrates. This report includes these results and the preliminary results on BSCCO superconductor thick film update.

II. $YBa_2Cu_3O_{7-x}$ Thick Films.

$YBa_2Cu_3O_{7-x}$ superconductor thick films had been made on different substrates with T_c between 43 and 90 K, as listed in Appendix I. Figure 1 shows the variation of T_c values of the $YBa_2Cu_3O_{7-x}$ thick films on different substrates obtained from previous work[1-17]. The films printed on Al_2O_3 based substrates, which included polycrystalline alumina and sapphire, showed lower T_c values and larger T_c variations. The films on alumina substrates had a higher relative magnetic susceptibility change than those on YSZ(Yttrium Stabilized Zirconia), MgO, 211 (Y_2BaCuO_5), and $SrTiO_3$ substrates[1]. This was due to the strong reaction between Al_2O_3 and the $YBa_2Cu_3O_{7-x}$ superconductor. The films printed on MgO and $SrTiO_3$ substrates also had large T_c variations. More consistent results, which had higher T_c values and smaller T_c value deviations, were obtained from the ZrO_2 based and 211 substrates. Ranking the substrates without a buffer layer, the best results from all of the reported literatures were on the ZrO_2 or 211 substrates, followed in order of increasing difficulty of preparation, MgO, spinel, $SrTiO_3$, Al_2O_3, and sapphire. Therefore, YSZ and 211 were used as substrate materials in this project. In order to compare the results on YSZ and 211 substrates, a new substrate made by $SrCO_3$, Nb_2O_5, and TiO_2 in the composition of $Sr_{0.875}(Ti_{0.75}Nb_{0.25})O_3$ was used as a substrate material in the project.

Cracks were found on $YBa_2Cu_3O_{7-x}$ superconductor thick films by Stastny[1]. This was due to the weak-link contact of the $YBa_2Cu_3O_{7-x}$ grains and thermal expansion mismatch between the $YBa_2Cu_3O_{7-x}$ thick film and

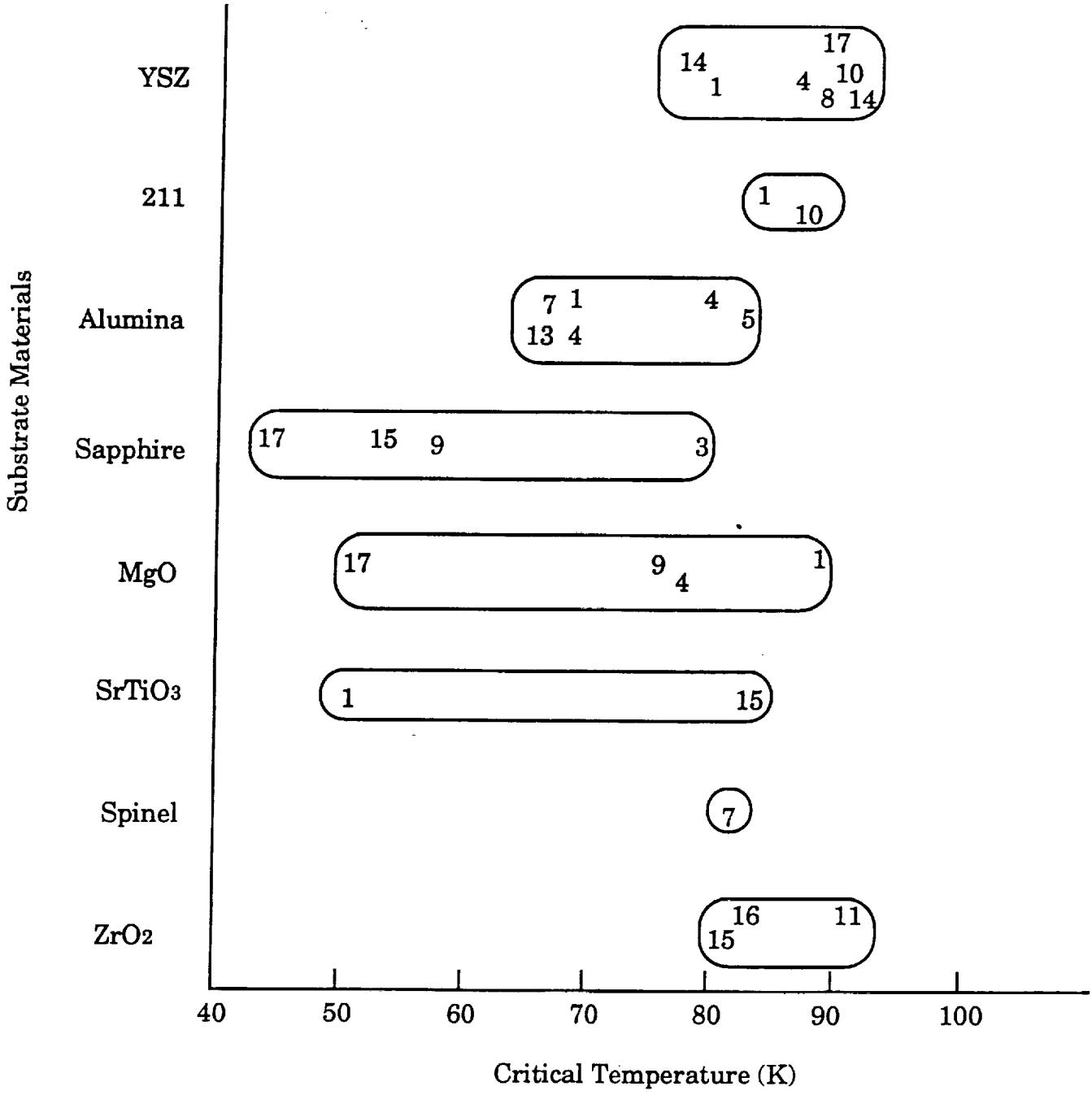

Figure 1: Variations of T_c value of $YBa_2Cu_3O_{7-x}$ superconductor thick films on different substrates. The numbers in the figure indicate the references used in this report.

substrates[1]. No or poor adhesion of the films were found when the films were printed on Al_2O_3 and YSZ substrates and fired at temperature below 950°C in O_2 atmosphere[3,13]. Adhesion between $YBa_2Cu_3O_{7-x}$ thick film and substrate was improved by adding Ag or Ag_2O to the superconductor[5,11]. Cracking was prevented when Ag was added to the $YBa_2Cu_3O_{7-x}$ thick films, owing to the strength imparted by the Ag[18]. Superconducting properties and density of the thick films were also enhanced by the Ag or Ag_2O addition[5,11,14]. In this project the $YBa_2Cu_3O_{7-x}$ thick films with different Ag_2O additions were prepared.

II.1 Experimental Procedure.

The YSZ, 211, and SNT substrates were prepared by tape casting. Because 211 and SNT substrates showed higher tan ∂ and/or poor mechanical strength, a polycrystalline alumina substrate was used to support these substrates. The 211 and SNT tapes were wet with toluene to bond them to Al_2O_3 substrates. The 211 substrate was sintered at 1150°C for 4 hours, whereas the SNT substrate was sintered at 1270°C for 4 hours. After sintering, both the 211 and SNT exhibited good adhesion to the alumina substrates. The YSZ substrate, with 8 wt% Y_2O_3, was sintered at 1520°C for 5 hours.

The $YBa_2Cu_3O_{7-x}$ raw powder was prepared by an ordinary solid state reaction method. High purity Y_2O_3, $BaCO_3$, and CuO were wet mixed and then calcined at 900°C for 5 hours. The calcined powder was annealed at 450°C for 12 hours before it was cooled down to room temperature. This calcination process was repeated for three times. After calcining, $YBa_2Cu_3O_{7-x}$ powder was ground, and then mixed with 10 to 30 wt% Ag_2O. $YBa_2Cu_3O_{7-x}$ paste was prepared by mixing the powder with a liquid organic medium. Before the paste was prepared, any interactions between $YBa_2Cu_3O_{7-x}$ powder and the organic medium was observed by a leaching test. In the test, 4 g of the powder was mixed with 4 g of a

liquid organic medium. The mediums examined were propylene glycol, terpineol, ethanol, toluene, and trichloroethylene. After three days aging, propylene glycol became blue. This might be caused from the leaching of copper ions from the $YBa_2Cu_3O_{7-x}$ powder. However, trichloroethylene, toluene, ethanol, and terpineol remained clear. Therefore, terpineol, ethanol, and toluene were used as solvents in paste preparation. The $YBa_2Cu_3O_{7-x}$ paste was prepared by mixing the powder, terpineol, ethanol, and toluene in 30:5:1:1 ratios. In order to increase adhesion of the green film, 10 wt% of binder (Metoramic Science Inc., B73305), was added to the paste.

After the substrates and $YBa_2Cu_3O_{7-x}$ paste were prepared, the films were deposited on the substrate by printing the paste through a 200 mesh stainless steel screen. Two kinds of patterns, single and multi-lead, were printed on the substrates. The single sample size was 1 cm wide and 4 cm long. The multi-lead sample had 15 lines, as shown in Figure 2. The size of each line was 20 mils width and 1500 mils length. The space between each line was 20 mils.

Films were sintered at 900 to 990°C for 5 minutes to 4 hours, in oxygen atmosphere. Electroding conditions, as determined in the previous project (Contract No. NAG-1-820), were used to apply the electrodes to the thick films.

Critical temperature of the sample showing zero resistance, T_c, was measured by four-point method. The T_c of the single film was measured with a constant current of 1 mA. The multi-lead sample's T_c was measured at 100 μA current. The J_c of the films, both single and multi-lead type, were measured at 1 μV /cm level at 77K. Film thicknesses were measured by Tencor, Alpha-step 200. SEM was used to observe the microstructure of the film.

II.2 Results and Discussions.

II.2.1 $YBa_2Cu_3O_{7-x}$ plain films.

$YBa_2Cu_3O_{7-x}$ thick films printed on 211/Al_2O_3 substrates showed poor adhesion to the substrates when they were fired at temperatures lower than 940°C. The samples were composed of the 211 green phase after being fired at temperatures higher than 940°C. Adding Ag_2O to the $YBa_2Cu_3O_{7-x}$ films

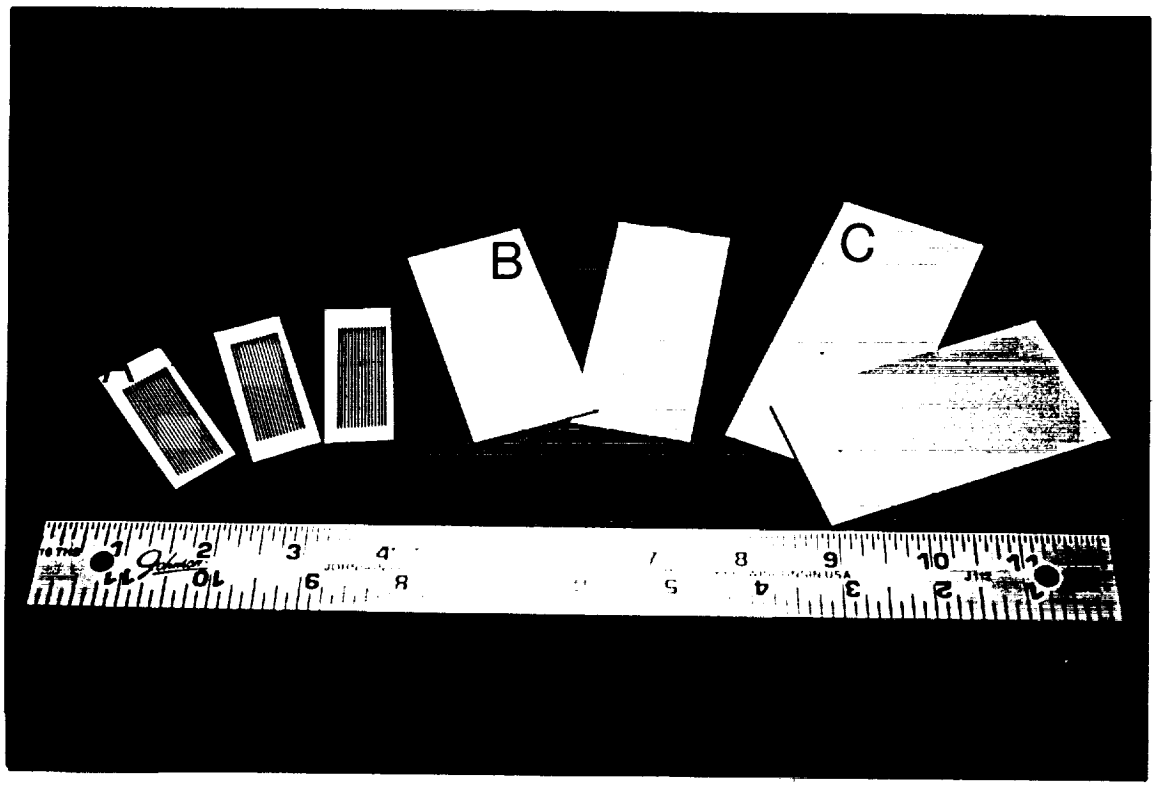

Figure 2: Multiple-lead $YBa_2Cu_3O_{7-x}$ superconductor samples (A), Sintered YSZ substrates (B), and YSZ green tapes (C).

improved their adhesion to the substrates. When 30 wt% Ag_2O was added to the films, $YBa_2Cu_3O_{7-x}$ superconducting thick films with good adhesion to the $211/Al_2O_3$ substrates were obtained. The $YBa_2Cu_3O_{7-x}$ films showed zero resistance at 80K with 1 mA measuring current, as listed in Table 1.

Table 1: The preparation conditions and properties of $YBa_2Cu_3O_{7-x}$ screen printed thick films on $211/Al_2O_3$ and SNT/Al_2O_3 substrates.

Substrate	Sintering Temp.	Sintering Time	T_c(K)	J_c(A/cm^2)	Ag(%)
$211/Al_2O_3$	900°C	4 hours	~80	-	30
$211/Al_2O_3$	910°C	2 hours	~80	-	30
$211/Al_2O_3$	920°C	1 hours	80	0.2	30
$211/Al_2O_3$	920°C	2 hours	80	1.0	30
SNT/Al_2O_3	950°C	10 min.	80	-	20
SNT/Al_2O_3	950°C	20 min.	82.6	1.8	20
SNT/Al_2O_3	950°C	10 min.	80.9	1	20

Films fired on the SNT/Al_2O_3 substrates had better adhesion than those fired on $211/Al_2O_3$ substrates. Smaller additions of Ag_2O were necessary for films fired on SNT/Al_2O_3 substrates because of improved film adhesion to the substrates. The T_c and J_c values of the $YBa_2Cu_3O_{7-x}$ films on SNT/Al_2O_3 substrates are listed in Table 1. These films had T_c values between 80 and 82.6 K at 1 mA measuring current. The highest J_c of the films on the SNT/Al_2O_3 substrates was 1.8 A/cm^2, which was fired at 950°C for 20 minutes.

YSZ substrates provided the best adhesion to the $YBa_2Cu_3O_{7-x}$ thick films among the three kinds of the substrates used in this project. Table 2 lists the T_c and J_c values of $YBa_2Cu_3O_{7-x}$ thick films printed on YSZ substrates. Ten or twenty weight percent of Ag_2O was added to the films. The films with 10 wt%

Ag_2O had T_c values between 81.2 and 86.1 K and J_c values between 2.6 and 15.2 A/cm^2. The T_c values of the films prepared at same conditions varied with the film thickness. Since a constant current was applied during measuring, a thicker sample had lower current density than that of a thinner sample. Higher T_c values were obtained from the thicker samples which were subjected to lower current density[19]. Samples had higher J_c values when their film thicknesses were in the range between 18 and 30 μm. The superconducting properties, T_c and J_c, of the samples were enhanced by increasing the silver content. When 20 wt% of Ag_2O was added to the $YBa_2Cu_3O_{7-x}$ thick film, the T_c value of the film was 85.8 K or higher. A J_c value of 50.4 A/cm^2 was obtained from a 20 wt% Ag_2O sample fired at 990°C for 10 minutes.

Currently, the influence of adhesion and silver on the superconducting properties of $YBa_2Cu_3O_{7-x}$ thick film and the thickness on the J_c values of the films are not clear and still under investigation.

II.2.2 $YBa_2Cu_3O_{7-x}$ multiple-lead film.

Multiple-lead thick films with 10 wt% Ag_2O were fabricated on YSZ substrates. The film fired at 980°C for 10 minutes had a T_c value of 82 K at 100 μA measuring current as shown in Figure 3. The J_c of each line at 77 K was 0.9 A/cm^2. The T_c of this sample was in the same range as the single samples fired at same conditions. The J_c of the film, however, was about five times lower than the single sample. The multiple-lead film fired at 970°C for 60 minutes was not in a superconducting state at 77 K with a 100μA measuring current. When the measuring current decreased to 10 μA, the sample showed zero resistance at 80.2 K. This was because of relatively low J_c values of the sample. The sample fired at 970°C for 1 hour had more serious cracking than the sample fired at 980°C for 10 minutes, as shown in Figure 4. The cracking yielded lower T_c and J_c values than those of the former sample, although it had a more dense film than the former. Since increasing the silver addition in the $YBa_2Cu_3O_{7-x}$ thick film was found to

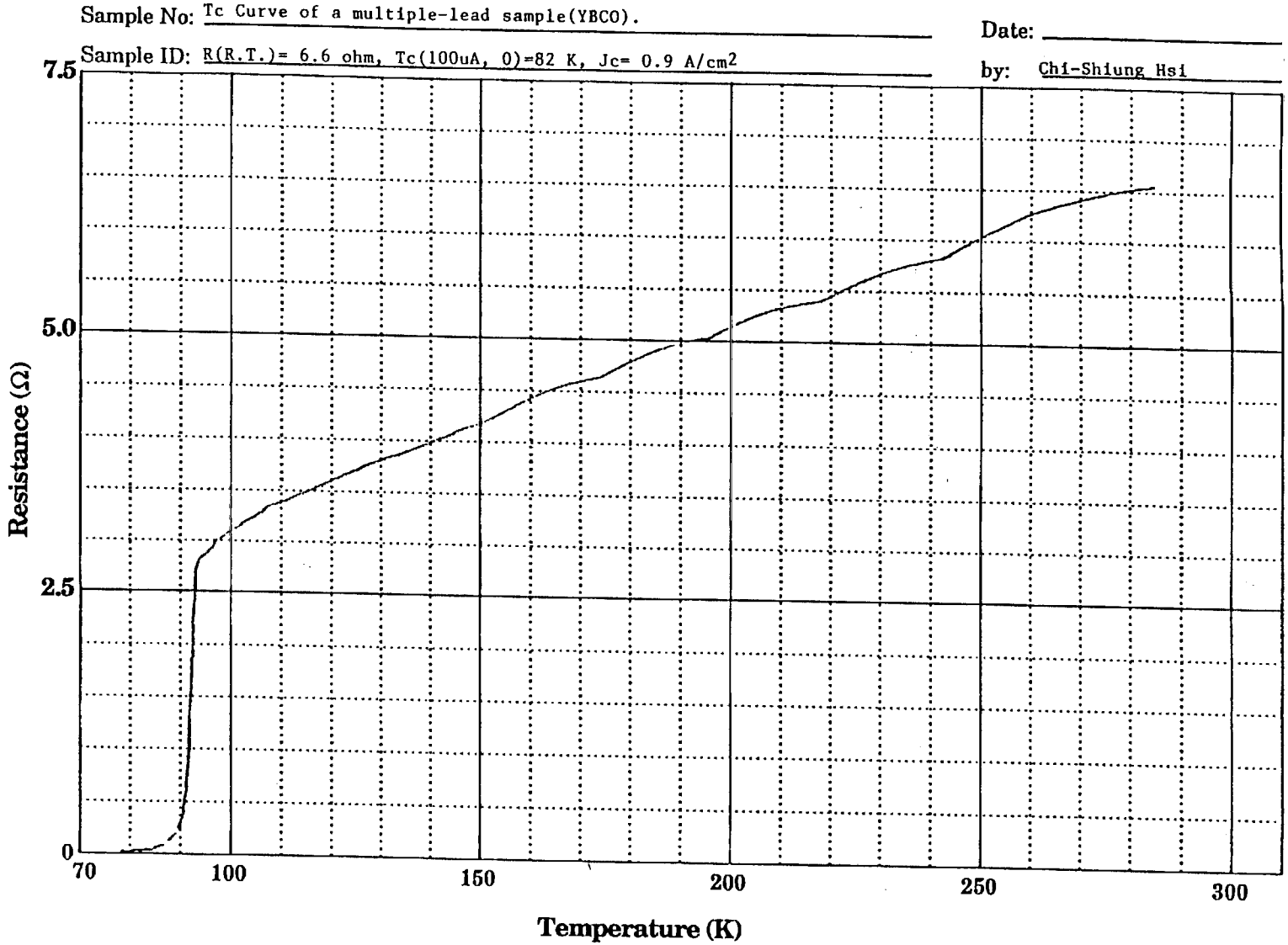

Figure 3: T_c curve of a $YBa_2Cu_3O_{7-x}$ multiple-lead sample. The resistance was measured at a 100 μA constant current.

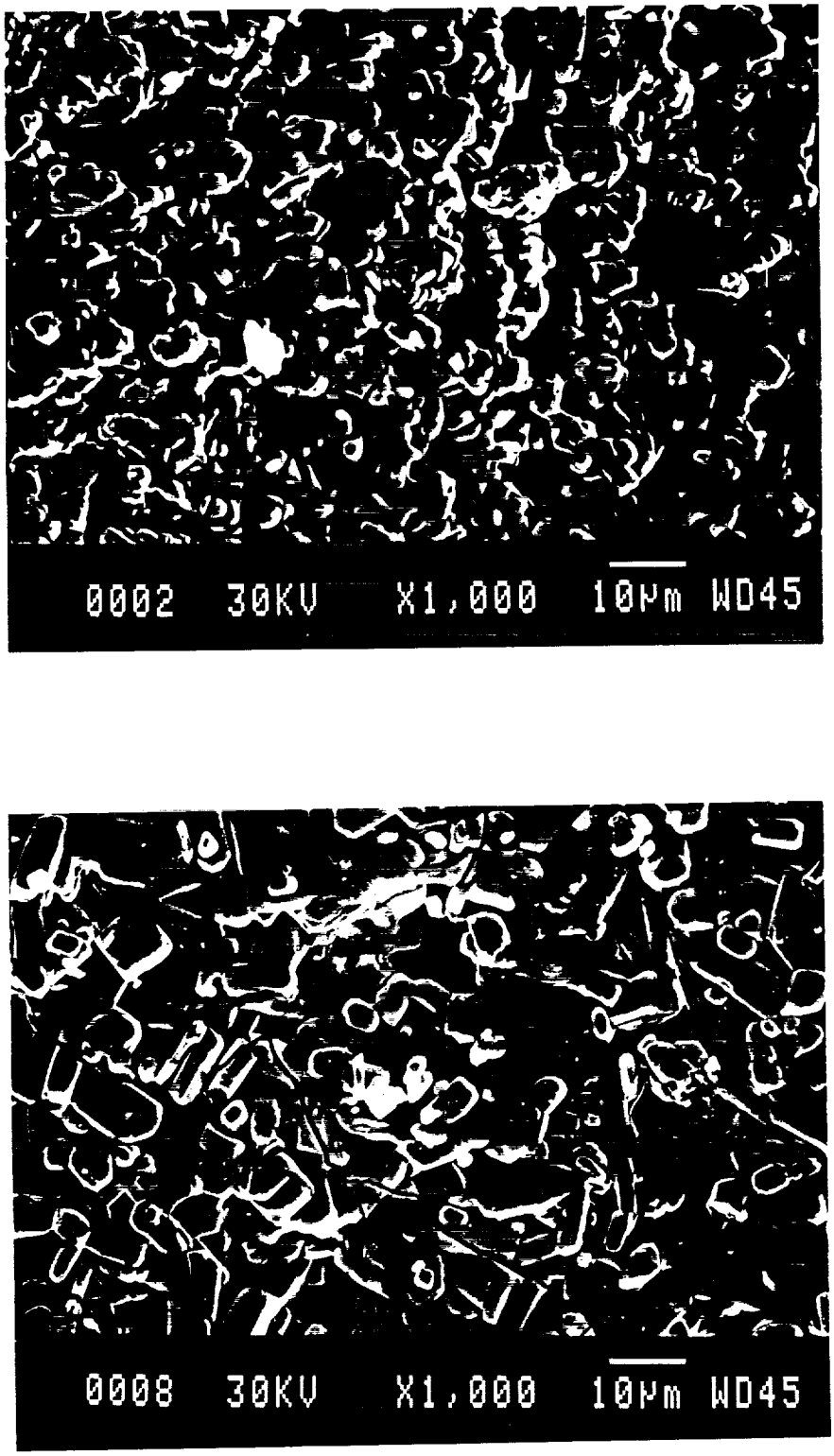

Figure 4: Microstructures of multiple-lead $YBa_2Cu_3O_{7-x}$ superconductors fired at 980°C for 10 minutes (top) and 970°C for 1 hour (bottom).

enhance the superconducting properties of the films, $YBa_2Cu_3O_{7-x}$ multiple-lead samples with 20 wt% Ag_2O or more will be made in the future.

Table 2: The preparation conditions and properties of $YBa_2Cu_3O_{7-x}$ screen printed thick films on YSZ substrates.

Sintering Temp.	Sintering Time	T_c(K)	J_c(A/cm^2)	Thickness	Ag(%)
950°C	1 hour	82.4	2.6	24 μm	10
970°C	10 min.	83.7	3.3	30 μm	10
970°C	1 hour	84.0	15.2	18 μm	10
970°C	1 hour	84.9	6.1	29 μm	10
980°C	10 min.	82.4	4.6	14 μm	10
980°C	10 min.	84.4	1.8	54 μm	10
980°C	30 min.	84.9	11.9	18 μm	10
980°C	30 min.	81.2	2.7	13 μm	10
990°C	5 min.	86.1	8.4	23 μm	10
990°C	10 min.	85.0	7.72	21 μm	10
990°C	10 min.	86.4	50.4	12 μm	20
960°C	10 min.	85.8	-	-	20

III. BSCCO Thick Films.

Phase transformation of BSCCO superconductor from high-T_c phase (2223) to low-T_c phase (2212) makes fabrication of BSCCO thick films more complex than that of Y-based thick film. Different compositions of lead doped BSCCO powders have been used in thick film processes, as listed in Appendix II. Because long heat treatment time is necessary to obtain pure 2223 phase thick films and interactions occur between the BSCCO material and the substrate, a

pure 2223 phase BSCCO powder is preferred to be used as a raw material to make a paste in the screen printing process. An undesirable insulating material (yellow-green in color) was found in the films fired on sapphire and YSZ substrate[17]. Both single crystal and polycrystalline MgO substrates were noted to be the best substrate materials for BSCCO thick films[17,20,21,23].

III.1 Experimental Procedure.

Two kinds of BSCCO powders of 2223 composition were prepared; i.e., (1) solid state reaction and (2) oxalate co-precipitation. In the solid state reaction method, Bi_2O_3, $SrCO_3$, $CaCO_3$, CuO, and PbO were mixed in distilled water and then dried at 110°C for 12 hours. The dry powder was calcined at 850°C for 30 hours, cooled to room temperature and crushed in a mortar and pestle. The powder was calcined with these conditions for four times before it was made into a paste. In the oxalate co-precipitation process, a clear precursor solution was prepared by mixing bismuth acetate, calcium acetate, strontium acetate, copper acetate, and lead subacetate in a methanol solution. Acetic acid and ammonium hydroxide were used to adjust the pH value of the solution. The precursor solution was slowly poured into a stirring oxalic acid / methanol solution, which produced a BSCCO oxalate co-precipitant. The co-precipitant was dried in a vacuum dryer for 8 hours. Dried BSCCO oxalate was calcined at 600°C for 6 hours to burn off the oxalate hydrocarbons. After the oxalate burned off, the BSCCO powder was further calcined at 830°C for 24 hour for 2 times.

A BSCCO paste was prepared by mixing BSCCO calcined powder with terpineol, ethanol, and toluene in 30:7:1:1 ratios. BSCCO thick films were printed on the MgO polycrystalline substrate by the same procedure used in the $YBa_2Cu_3O_{7-x}$ thick film process. Screen printed BSCCO thick films were fired at temperatures between 830 to 855°C for different times.

III.2 Results and Discussion.

III.2.1 Powder Characterization.

BSCCO powders prepared by the solid state reaction and co-precipitation methods were characterized by measuring the T_c curve of a sintered pellet and the X-ray diffraction patterns of powders. Figure 5 shows the T_c curve of a sintered pellet prepared from the solid state reaction powder. The pellet had a T_c of 103 K. Two steps were found in the T_c curve between the onset and offset temperatures. Both low and high-T_c phases were found in the four times calcined oxide powder, as shown in Figure 6. Only one step was found in the T_c curve of the oxalate prepared pellet, as shown in Figure 7, indicating a homogeneous, single phase 2223 material. This sample had a T_c=105.7 K and J_c= 141 A/cm^2. Presently, different calcination conditions for the oxalate co-precipitated powder are under investigation in order to achieve the best calcination conditions for this powder.

III.2.2 BSCCO Thick Film.

Figure 8 shows the T_c curve of a BSCCO screen printed thick film prepared by four times calcined powder. The film was fired at 845^{0}C for 1 hour. Two steps, as found in the T_c curve of the four times calcined pellet, were observed from this curve. The film was not in the superconducting state at 77 K with 1 mA measuring current. When the measuring current was decreased to 0.62 mA, the film show zero resistance at 77 K. Therefore, this film had a relatively low critical current density (J_c) . So far, only a few results were obtained from Bi-based thick films. The firing conditions and properties of BSCCO thick films prepared by solid state reaction and oxalate co-precipitation will be included in a future report.

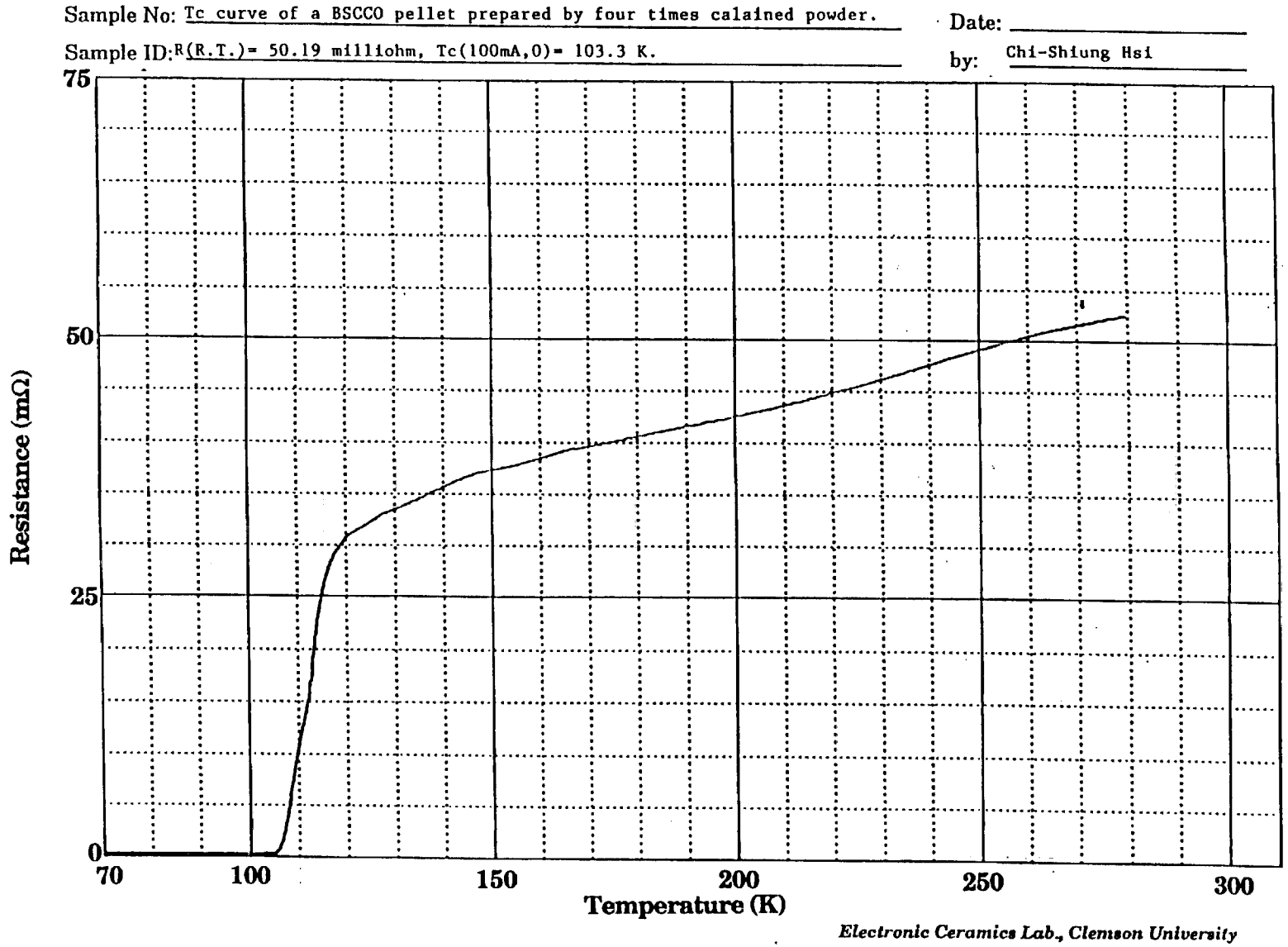

Figure 5: T_c curve of a BSCCO superconductor sintered pellet. The pellet was prepared by solid state reaction powder.

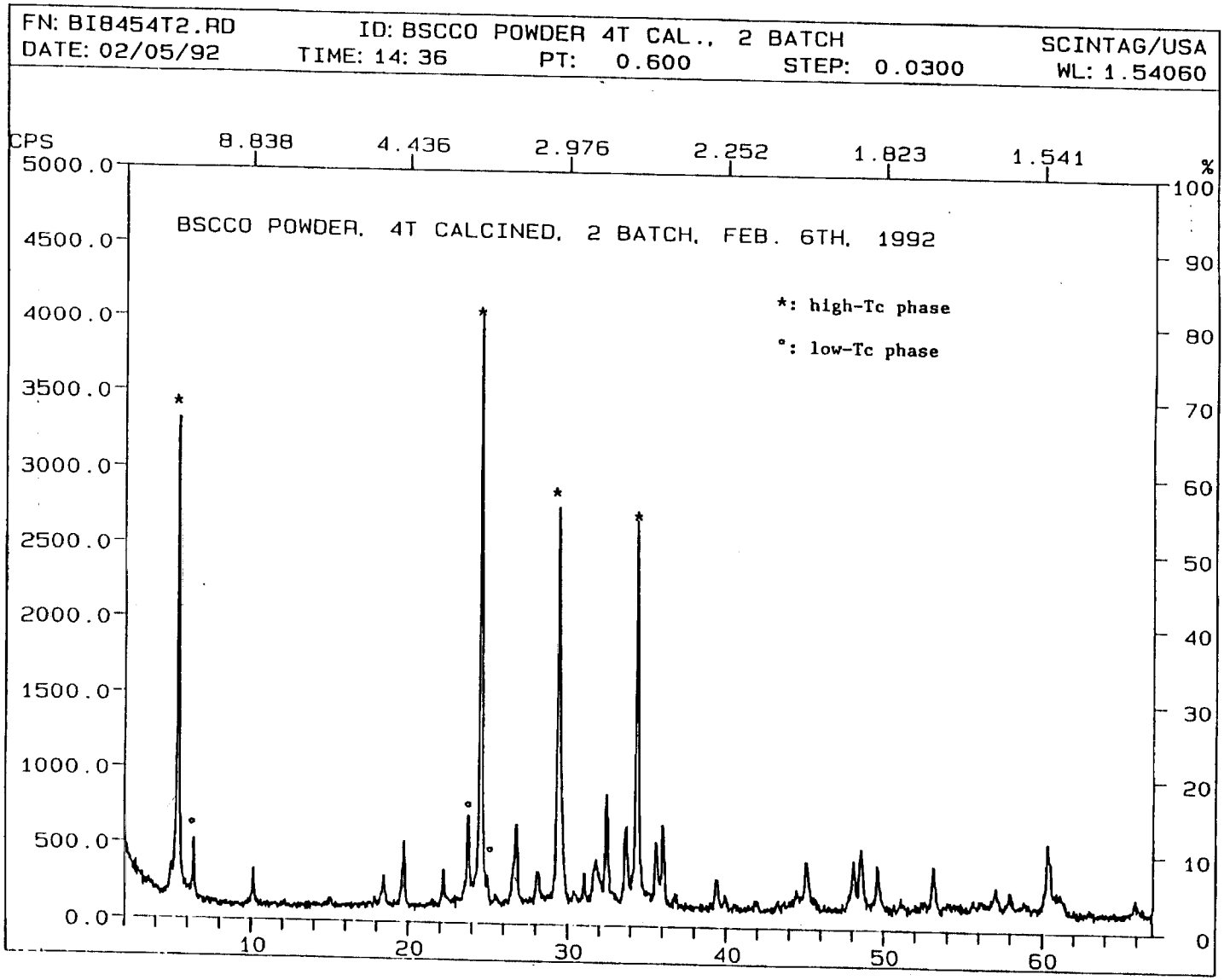

Figure 6: X-ray diffraction pattern of a solid state reaction powder after four times calcined at 845°C for 30 hours.

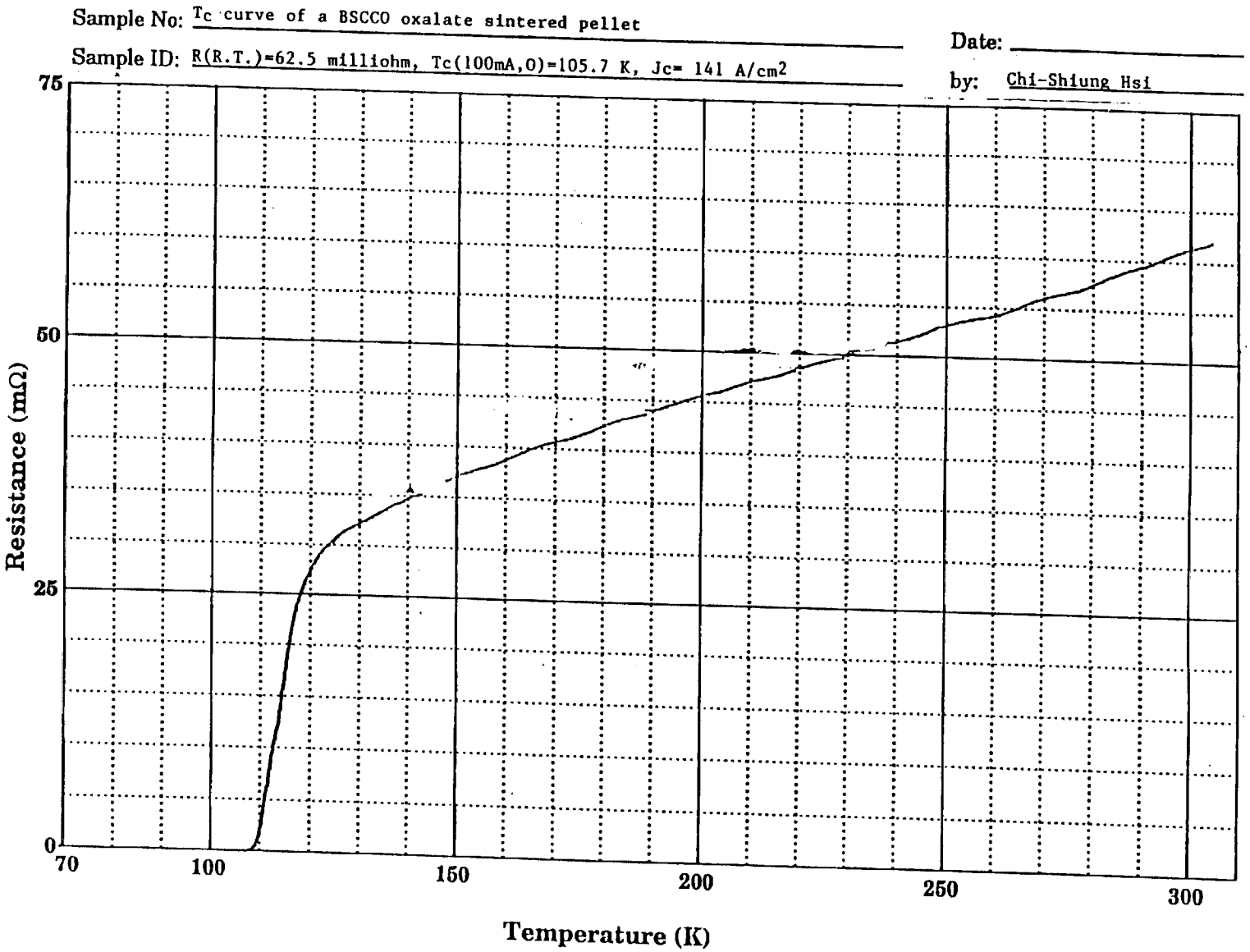

Figure 7: T_c curve of a BSCCO superconductor sintered pellet. The pellet was prepared by oxalate co-precipitated powder and sintered at 850°C for 30 hours.

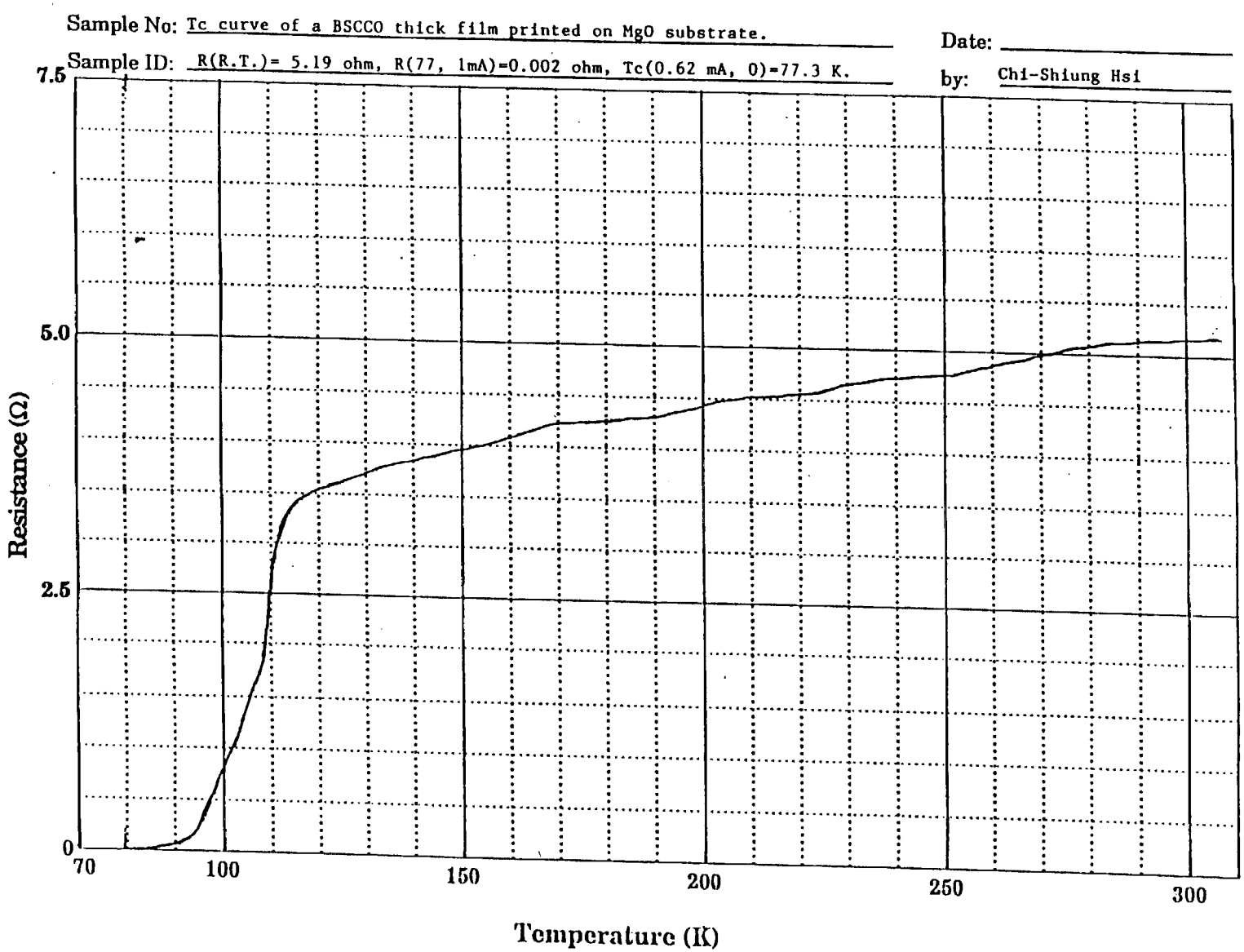

Figure 8: T_c curve of a BSCCO thick film printed on a MgO substrate. The film was annealed at 845°C for 1 hour.

IV. Summary.

1. $YBa_2Cu_3O_{7-x}$ superconducting screen printed thick film with T_c= 86.4 K and J_c= 50.4 A/cm^2 was prepared on YSZ substrate.

2. Mutiple-lead $YBa_2Cu_3O_{7-x}$ superconducting thick film with T_c= 82 K was deposited on YSZ substrate. The J_c of the sample, however, was relatively lower than the plain samples.

3. A pure high-T_c BSCCO (2223) powder was obtained via oxalate co-precipitating process.

References

1. P. Stastny, R. Kuzel, and V. Skacel, J. Less-Common Metals, 164-165, 464-469, 1990.
2. M. V. S. Lakshmi, K. Ramkumar, and M. Satyam, J. Mater. Sci., 26, 4092-4094, 1991.
3. R. C. Budhani, S. M. Tzeng, H. J. Doerr, and R. F. Bunshah, Appl. Phys. Lett., 51, 1277-1279, 1987.
4. N. L. Corah, Jr., R. L. Wahlers, S. J. Stein, I. Perez, J. Schwegler, G. H. Myer, and J. E. Crow, ISHM '89 Proceeding.
5. C. Wu, Y. Tzeng, R. P. Hunt, M. A. Belser, and T. A. Roppel, J. Electrochem. Soc., 136, 1570-1571, 1989.
6. M. Itoh and H. Ishigaki, Jpn. J. Appl. Phys., 27, L420-L422, 1988.
7. N. P. Bansal, R. N. Simons, and D. E. Farell, Appl. Phys. Lett., 53, 603-605, 1988.
8. M. Senda and O. Ishii, J. Appl. Phys., 69, 6586-6589, 1991.
9. J. Tabuchi and K. Utsumi, Appl. Phys. Lett., 53, 606-608, 1988.
10. K. Yoshiara, K. Kagata, S. Yokoyama, T. Hiroki, H. Higuma, T. Yamazaki, and K. Nakahigashi, Jpn. J. Appl. Phys., 27, L1429-L1494, 1988.
11. I. Dhingra, G. K. Padam, S. Singh, R. B. Tripathi, S. M. U. Rao, D. K. Suri, K. C. Nagpal, and B. K. Das, J. Appl. Phys., 70, 1575-1579,1991.
12. A. Bailey, S. L. Town, G. Alvarez, G. J. Russell, and K. N. R. Taylor, Physica C, 161, 347-350, 1989.
13. N. P. Bansal, R. N. Simons, and D. E. Farrell, High T_c Superconductor I, Am. Ceram. Soc., p 474-482, 1989.
14. Y. Matsuoka, E. Ban, and H. Ogawa, J. Phys. D: Appl. Phys., 22, 564-565, 1989.
15. J. M. Aponte and M. Octavio, J. Appl. Phys., 66, 1480-1482, 1989.
16. K. Przybylski, J. Koprowski, J. Oblakowski, and M. Wierzbicka, J. Less-Common Metals, 164-165, 470-477, 1990.
17. T. Tabuchi, Y. Shimakawa, A. Ochi, and K. Utsumi, High T_c Superconductor I, Am. Ceram. Soc.,p 464-473, 1989.
18. S. E. Dorris, M. T. Lanagan, D. M. Moffatt, H. J. Leu, C. A. Youngdahl, U.

Balachandran, A. Cazzato, D. E. Bloomberg, and K. C. Gretta, Jpn. J. Appl. Phys., 28, L1415-1416, 1989.

19. L. F. Goodrick and S. L. Bray, Cryogenics, 30, 667-677, 1990.
20. T. Brousse, R. Retoux, G. Poullain, J. Provost, H. Murray, D. Bloyet, and B. Raveau, Appl. Phys. A, 49, 217-220, 1989.
21. A. Uusimaki, I. Kirschner, J. Levoska, J. Levoska, G. Zsolt, Gy. Kovacs, T. Projesz, I. Dodony, S. Leppavuori, E. Lahderanta, and R. Laiho, Cryogenics, 30, 593-598, 1990.
22. T. Hashimoto, T. Kosaka, Y. Yoshida, K. Fueki, and H. Koinuma, Jpn. J. Appl. Phys., L384-L386, 1988.
23. K. Hoshino, H. Takahara, and M. Fukutomi, Jpn. J. Appl. Phys., L1297-L1299, 1988.
24. T. Nakamori, H. Abe, Y. Takahashi, T. Kanamori, and S. Shibata, Jpn. J. Appl. phys., L649-L651, 1988.

Appendix I. Literature reviews of YBCO screen printed thick films.

Substrate	Binder	Firing Cond.	T_c(K)	J_c(A/cm^2)	Film Thickness(μm)	Reference
211	terpinoel	930-960°C	83	-	50	1
MgO		10 min.	88	-		
YSZ		O_2	79	120		
$SrTiO_3$			50	-		
Al_2O_3			68			
Al_2O_3/Ag	Triethanolamine	950°C		0.012	100	2
		10 min.				
Al_2O_3	Du-Pont 9180	1000°C	70	-	10	3
Sapphire		30 min	79	9		
		O_2				
96% Al_2O_3	-	980 °C	68	90*	30-50	4
99.6% Al_2O_3		air	79	5*		
MgO			77	230*		
YSZ			86	30*		
Al_2O_3		1040°C	82	12.4	150	5
		10 min.				
		O_2				
Al_2O_3/		925°C	46		25	6
Y-Ba-Cu-O		1h./ air	88.5		100	

Substrate	Binder	Firing Cond.	T_c(K)	J_c(A/cm^2)	Film Thickness(μm)	Reference
Al_2O_3 Spinel		1000°C 15 min. O_2	66 81	-		7
YSZ/Ag		1050°C 10 min/O_2	88.5	700		8
YSZ MgO Sapphire		970-990°C 1-6 min. O_2	89 75 57	70	40 40 40	9
211 YSZ	diethylene terpineol	950°C 1 hour	86 85	3000	40 40	10
ZrO_2(MgO)	ethyl - cellulose	980°C 1-2 h/ O_2	90	20	25	11
Al_2O_3		1000°C 15 min./ O_2	66	-	40	13
YSZ		980°C 6min O_2	90(27% Ag) 87(Ag_2O) 77(pure)	190 3.5 0.013	- - -	14

Substrate	Binder	Firing Cond.	T_c(K)	J_c(A/cm^2)	Film Thickness(μm)	Reference
$SrTiO_3$		970-1000°C	82	10	-	15
Sapphire			52	-	-	
$Zr(Ca)O_2$			80	0.1	-	
ZrO_2		1000°C 6 min./ O_2	82	22	-	16
YSZ		970-990°C	89	70	40	17
MgO		1-6 min	50	-	10	
Sapphire			43	-	10	

*: J_c was measured at 4.2 K.

Appendix II. Literature reviews of BSCCO screen printed thick films.

Substrate	Film Composition	Firing Cond.	T_c(K)	J_c(A/cm^2)	Reference
MgO	$Bi_{1.6}Pb_{0.4}Sr_{1.6}Ca_{2.4}Cu_3O_{10}$	865°C, 5h	101	10	20
MgO(100)	$Bi_{1.9}Pb_{0.4}Sr_{1.9}Ca_{2.1}Cu_{3.2}O_{10}$	895°C, 2h- 850°C, 80h	105	2000	21*
MgO(100)	$Bi_2Sr_2Ca_2Cu_3O_{10}$	900°C, 5 min.	62	-	17
YSZ		900°C, 1h	72	-	
YSZ	$Bi_2Sr_2Ca_2Cu_3O_{10}$	850°C, 1h	68	-	22
MgO(100)	$Bi_2Sr_2Ca_2Cu_3O_{10}$	885°C, 1h- 872°C, 72h	107	-	23*
Ag		880°C, 10 min.	76	-	
MgO(100)	$Bi_2Sr_2Ca_2Cu_3O_{10}$	890°C,1h- 870°C, 40h	<80	-	24*

*: Samples were annealed by two steps firing program.

Omit

Part II

Semi-Annual Report

SUPERCONDUCTIVITY DEVICES: COMMERCIAL USE OF SPACE

An Acetate Precursor Process for BSCCO (2223) Thin Films and Coprecipitated Powders

Submitted to

National Aeronautics and Space Administration

Langley Research Center

Submitted by

LaDawn McIntyre

Principal Investigator

Gene H. Haertling

Department of Ceramic Engineering

Clemson University

Contract No. NAG-1-1301

April 1992

INTRODUCTION

Since the discovery of high temperature superconducting oxides much attention has been paid to finding better and useful ways to take advantage of the special properties exhibited by these materials. One such process is the development of thin films for engineering applications. Another such process is the coprecipitation route to producing superconducting powders.

THIN FILMS

Thin films are of indispensable use in applied electronics, and have been prepared with a variety of vacuum and non-vacuum techniques. Some of the vacuum technology techniques include magnetron sputtering, co-evaporation, ion beam sputtering and laser deposition. Some non-vacuum techniques include screen printing, spray pyrolysis, spin coating and dip-coating. The dip coating technique is of particular interest due to its many advantages. This process is more economical, faster, and simpler than the vacuum processes. The coating chemistry can easily be controlled and thicker films are possible. There are very few limits to the size and shape of the dip coated device and double sided deposition is possible. Dip coating does have disadvantages. Films made by this process are easily contaminated with foreign debris, and have a porous structure.

Bismuth based superconducting thin films have been prepared via non-vacuum techniques with solutions of acetates,[1] alkoxides,[2] ethylhexanoates,[3] naphthenates,[4,5] and nitrates.[6] It was decided to explore the acetate route as means to produce a (Bi,Pb)-Sr-Ca-Cu-O coating film. A lead

doped Bismuth system was chosen over the Bi-Sr-Ca-Cu-O system as the addition of lead helps to form the high T_c=110K (2223) phase.[7-11]

Coprecipitation

A coprecipitation route to producing superconducting powders has many advantages over the solid state oxide route. It is relatively easy to produce powders of high purity and of a fine grain size, whereas the solid state route requires ball milling to produces such fine powders, and the ball milling contaminates the powder. Powders derived from coprecipitation have a much higher precursor reactivity, thus reducing the number and duration of calcines often needed in the solid state systems.[12] Coprecipitation methods also circumvent problems in obtaining high purity oxides of the appropriate particle size to begin the solid state process. Problems encountered in using the coprecipitation route include 1) first producing an appropriate solution, and 2) possible separate precipitation of the chemicals. The precipitation system and conditions must be carefully controlled to obtain reproducibility.[12]

Since it was decided to explore a dip-coating process with a solution of acetates, it was also deemed convenient to use this same solution for a coprecipitation process. A bulk material was made and tested as a way of evaluating the usefulness of this method for applications in thin section tape casting and screen printing.[13-14]

OBJECTIVES

The objectives of this work were (1) to develop an acetate solution for use in dip coating and chemical

coprecipitation, (2) to produce and evaluate thin films of said solution, and (3) to coprecipitate the same solution and determine the viability of this powder production route for use in thin-section tapecasting and screen printing.

EXPERIMENTAL PROCEDURE

THE ACETATE SOLUTION

$Bi(COOCH_3)_3$, $C_4H_{10}O_8Pb$, $Sr(COOCH_3)_2$, $Ca(COOCH_3)_2 \cdot H_2O$, and $Cu(COOCH_3)_2 \cdot H_2O$ were batched such that the final product would be of the composition $(Bi_{1.6}Pb_{0.4})Sr_{1.9}Ca_{2.05}Cu_{3.05}$ in order to produce the high T_c (or 2223) phase. The percent oxide values used are shown in Table 1 and a batch sheet for a one gram oxide batch is shown in Table 2. Powders of the BiAc, PbSAc, SrAc, and CaAc were placed in a glass beaker along with 3.82g of an 80% acetic acid/20% water solution per gram of oxides. The system was stirred until a clear solution was obtained. Methanol (4.00g per gram of oxides) was then added to the existing solution. Powdered CuAc was added next, followed by 1.30g ammonium hydroxide per gram oxides. This system was stirred until a clear blue solution was obtained. The solution was then brought to a pH of approximately 7 with 0.30g of acetic acid per gram of oxides. This process yielded an 8.7% oxide solution. A flow chart of this process is shown in Figure 1.

THE THIN FILMS

The silver substrate was cleaned, rinsed in distilled water, dipped in zirconium acetate and then rinsed again in preparation for dipping. The original solution was diluted with methanol to 7.0% oxides, and then the substrate was

slowly dipped into the solution by hand. The film was allowed to dry for two minutes at room temperature and then introduced into a furnace held at temperatures ranging from 200°C to 600°C. This dipping, drying and firing process was repeated five to ten times. The resulting films were observed under a Zeiss optical microscope in order to determine which firing temperatures produced useful thin films. Films deemed to be of reasonable quality were analyzed for phase content with X-ray diffraction using Cu K_α radiation. The results of further heat treatments and subsequent tests and measurements are unavailable at this time. A flow chart of this process is located in Figure 2.

COPRECIPITATED MATERIAL

The original solution was batched for 25g of oxides. This solution was slowly added to 50g of oxalic acid dissolved in 200g of methanol with constant vigorous stirring. This system was then dried overnight at 100°C. The existing organics were burned out in an alumina crucible with a ramp of 1.7°C/min, a set point of 600°C and a dwell time of 6 hours. The resulting powder was then pressed at 5,120 lbs/in^2 into a square pellet and calcined once or twice in air. The calcine schedule includes a 1.7°C ramp with a final temperature of 830°C and a dwell time of 24 hours. The calcined material was then ground with a mortar and pestle and passed through a 140 mesh screen. The powder was then pressed into a pellet at 5,120 lbs/in^2. A ramp of 1.7°C, a set point of 845°C and a dwell time of 30 hours was used to sinter the pellet in air. The pellet was tested for the Meissner effect and then a thin slice was cut from the pellet and electroded with silver paste (C8710 from Heraeus Inc., Cermalloy Division) which was fired

on at 845°C for 18 minutes in air. The critical current density and the critical temperature were measured for both the once calcined and twice calcined material using the standard four point method. The resistance was measured with a Keithley Model 580 micro-ohmmeter with a sensitivity of $10^{-6}\Omega$. The critical current was measured with a 1μV per mm standard using a Keithley Model 197 Autoranging MicroVolt DMM. The samples were also examined by powder X-ray diffraction using Cu K_α radiation. A flow chart for this process is contained in Figure 3.

RESULTS AND DISCUSSION

THIN FILMS

The films fired at 350°C and 400°C were the only ones deemed to be of reasonable quality and were therefor subjected to further testing. These five layer films had obvious flaws as viewed under an optical microscope, although not nearly as many flaws as the films processed at higher temperatures. Photomicrographs of these films are included in Figure 4. X-ray diffraction (XRD) data for these films can be found in Figure 5. The XRD data were inconclusive, as only the silver substrate was clearly present. Further tests of films with more layers is necessary to provide a conclusive study of this particular method.

MATERIAL FROM COPRECIPITATED POWDER

The final sintered pellets made of both the once calcined and twice calcined material were able to demonstrate the full Meissner effect. A T_c of 104.9 K, and a J_c of 20 A/cm^2 was obtained for the twice calcined material. A T_c of 104.3 K,

and a J_c of 8 A/cm^2 was obtained for the once calcined material. T_c curves are shown in Figures 6 and 7. XRD data can be found in Figure 8. The once calcined material contains the T_c=110 K ($Bi_2Sr_2Ca_2Cu_3$ or 2223) superconducting phase and the T_c=85 K ($Bi_2Sr_2CaCu_2$ or 2212) superconducting phase. The twice calcined clearly contains the 2223 phase and only very little of the 2212 phase. These results with only one or two calcines are similar to those in the literature[15-18] with three or more calcines. Since the behavior of a bulk material is often indicative of the behavior of the system if it is used in other applications, it would appear that this method of powder production is feasible for use in thin section tape casting and screen printing.

CONCLUSIONS

An acetate precursor process for use in thin film fabrication and a chemical coprecipitation route to Bismuth based superconducting materials has been developed. Data obtained from the thin film process were inconclusive to date and require more study. The chemical coprecipitation method of producing bulk material is a viable method, and is preferred over the previously used solid state route. This method of powder production appears to be an excellent route to producing thin section tape cast material and screen printed devices, as it requires less calcines than the oxide route to produce quality powders.

References

1. Zhuang, H., H. Kozuka, T. Yoko, and S. Sakka, (1990). "Preparation of Superconducting Bi-Sr-Ca-Cu-O Coating Films by the Sol-Gel Method Using an Aqueous Solution of Metal Acetates," *Jap. J. Appl. Phys.*, vol. 29, No. 9, July, pp. L1107-L1110.

2. Hirano, S., T. Hayashi, and H. Tomonaga, (1990). "Preparation of Superconducting Bi-Sr-Ca-Cu-O Films with Preferred Orientation through a Metal Alkoxide Route," *Jap. J. Appl. Phys.*, vol. 29, No. 1, January, pp. L40-L42.

3. Nasu, H., S. Makida, Y. Ibara, T. Kato, T. Imura, and Y. Osaka, (1988). "Preparation of $BiSrCaCu_2O_x$ Films with T_c > 77 K by Pyrolysis of Organic Acid Salts," *Jap. J. Appl. Phys.*, vol. 27, No. 4, April, pp. L536-L537.

4. Nasu, H., H. Nonogawa, A. Nozue, and K. Kamiya, (1990). "Preparation of Mostly Single High-T_c Phase Thin Films in Bi, Pb-Sr-Ca-Cu-O by Pyrolysis of Organic Acid Salts," *Jap. J. Appl. Phys.*, vol. 29, No. 3, March, pp. L450-L452.

5. Maruyama, T. and S. Higashi, (1989). "High-T_c Superconducting Bi-Pb-Sr-Ca-Cu-O Thin Films Prepared by Thermal Decomposition of Metallic Complex Salts," *Jap. J. Appl. Phys.*, vol. 28, No. 4, April, pp. L624-L627.

6. Nobumasa, H., K. Shimuzu, Y. Kitano, and T. Kawai, (1988). "Formation of a 100 K Superconducting Bi(Pb)-Sr-Ca-Cu-O Film by a Spray Pyrolysis," *Jap. J. Appl. Phys.*, vol. 27, No. 9, September, pp. L1669-L1671.

7. Yanagisawa, E., D. R. Dietderich, H. Kumakura, K. Togano, H. Maeda, and K. Takahashi, (1988). "Properties of a Pb-Doped Bi-Sr-Ca-Cu-O Superconductors," *Jap. J. Appl. Phys.*, vol. 27, No. 8, August, pp. L1460-L1462.

8. Endo, U., S. Koyama, and T. Kawai, (1989). "Composition Dependence on the Superconducting Properties of Bi-Pb-Sr-Ca-Cu-O," *Jap. J. Appl. Phys.*, vol. 28, No. 2, February, pp. L190-L192.

9. Kim, C. J., C. K. Rhee, H. G. Lee, C. T. Lee, S. J-L. Kang, and D. Y. Won, (1989). "The Formation of High-T_c Phase in Pb-Doped Bi-Sr-Ca-Cu-O System," *Jap. J. Appl. Phys.*, vol. 28, No. 1, January, pp. L45-L48.

10. Kim, C. J., C. K. Rhee, H. G. Lee, I. H. Kuk, J. M. Lee, I. S. Chang, C. S. Rim, P. S. Han, S. I. Pyun, and D. Y. Won, (1989). "Effects of the Pb Content on the Formation of the High-T_c Phase in the (Bi, Pb)-Sr-Ca-Cu-O System," *Jap. J. Appl. Phys.*, vol. 28, No. 7, July, pp. L1137-L1139.

11. Oota, A., K. Ohba, A. Ishida, A. Kirihigashi, K. Iwasaki, and H. Kuwajima, (1989). "Growth Process of the (2223) Phase in Pb-Added Bi-Sr-Ca-Cu-O," *Jap. J. Appl. Phys.*, vol. 28, No. 7, July, pp. L1171-L1174.

12. Reed, J. S., (1988). *Introduction to the Principles of Ceramic Processing*, John Wiley & Sons, New York.

13. Nakamori, T., H. Abe, Y. Takahashi, T. Kanamori, and S. Shibata, (1988). "Preparation of Superconducting Bi-Sr-Ca-Cu-O Printed Thick Films Using a Coprecipitation of Oxalates," *Jap. J. Appl. Phys.*, vol. 27, No. 4, April, pp. L649-L651.

14. Vilminot, S., S. El Hadigui, J. P. Kappler, J. C., Bernier, T. Dupin, R. Barral, and G. Bouzat, (1988). "Synthesis and Characterization of $YBa_2Cu_3O_{7-X}$ Ceramic Powders from an Oxalic Route," *British Ceramic Proceedings*, No. 40, March, pp. 15-18.

15. Iwai, Y., M. Takata, T. Yamashita, M. Ishii, and H. Koinuma, (1989). "Formation of the High-T_c Phase of $Bi_{1-x}Pb_xSr_{0.90}Ca_{1.10}Cu_{1.50}O_y$ ($0 \le x \le 0.05$)," *Jap. J. Appl. Phys.*, vol. 28, No. 9, September, pp. L1518-L1520.

16. Lee, S-G., K-S. Yi, C-Y. Park, and M-S. Jang, (1989). "Normal-State Resistivity of the (Bi/Pb)-Ca-Sr-Cu-Oxide System," *Jap. J. Appl. Phys.*, vol. 28, No. 11, November, pp. L1902-L1905.

17. Narumi, S., H. Ohtsu, I. Iguchi, and R. Yoshizaki, (1989). "Synthesis of 110 K Bi(Pb)-Ca-Sr-Cu-O Oxide Superconductors," *Jap. J. Appl. Phys.*, vol. 28, No. 1, January, pp. L27-L30.

18. Takayama-Muromachi, E., Y. Uchida, Y. Matsui, M. Onoda, and K. Kato, (1988). "On the 110 K Superconductor in the Bi-Ca-Sr-Cu-O System," *Jap. J. Appl. Phys.*, vol. 27, No. 4, April, pp. L556-L558.

Percent Oxide Calculations

Solution of Acetates

$Bi_{1.6}Pb_{0.4}Sr_{1.9}Ca_{2.05}Cu_{3.05}$

$$BiAc \rightarrow \frac{Bi_2O_3}{2[Bi(COOCH_3)_3]} = \frac{465.96}{772.22}(100\%) = 60.34\%$$

$PbSAc \rightarrow 78.6\%$ (*Experimental value obtained by this laboratory*)

$$SrAc \rightarrow \frac{SrO}{Sr(OOCCH_3)_2} = \frac{103.62}{205.71}(100\%) = 50.37\%$$

$$CaAc \rightarrow \frac{CaO}{Ca(CH_3COO)_2 \cdot H_2O} = \frac{56.08}{176.18}(100\%) = 31.83\%$$

$$CuAc \rightarrow \frac{CuO}{Cu(CH_3COO)_2 \cdot H_2O} = \frac{79.54}{199.65}(100\%) = 39.84\%$$

Table 1 Percent oxide calculations for batching the powder acetate precursors. With the exception of the lead acetate (PbSAc) the calculations are based on molecular weights.

Batch Information Sheet
For One Gram of Oxides in Final Solution
Final Composition $(Bi_{1.6}Pb_{0.4})Sr_{1.9}Ca_{2.05}Cu_{3.05}$

Oxide	Acetate Precursor	Molecular Wt. Oxide	Moles	Formula Wt.
Bi_2O_3	BiAc	465.96	1.6/2	372.77
PbO	PbSAc	223.19	0.40	89.28
SrO	SrAc	103.62	1.90	196.88
CaO	CaAc	56.08	2.05	114.96
CuO	CuAc	79.54	3.05	242.60
				Total
				1016.49

Precursor	(Weight %)/(% Oxide)= amount for 1g batch
BiAc	36.67/60.34= 0.608
PbAc	8.78/78.6= 0.112
SrAc	19.37/50.37= 0.385
CaAc	11.31/31.83= 0.355
CuAc	23.87/39.84= 0.599

Table 2 The batch information sheet for the acetate solution showing the amounts of each precursor needed to produce one gram of oxides in the final batch.

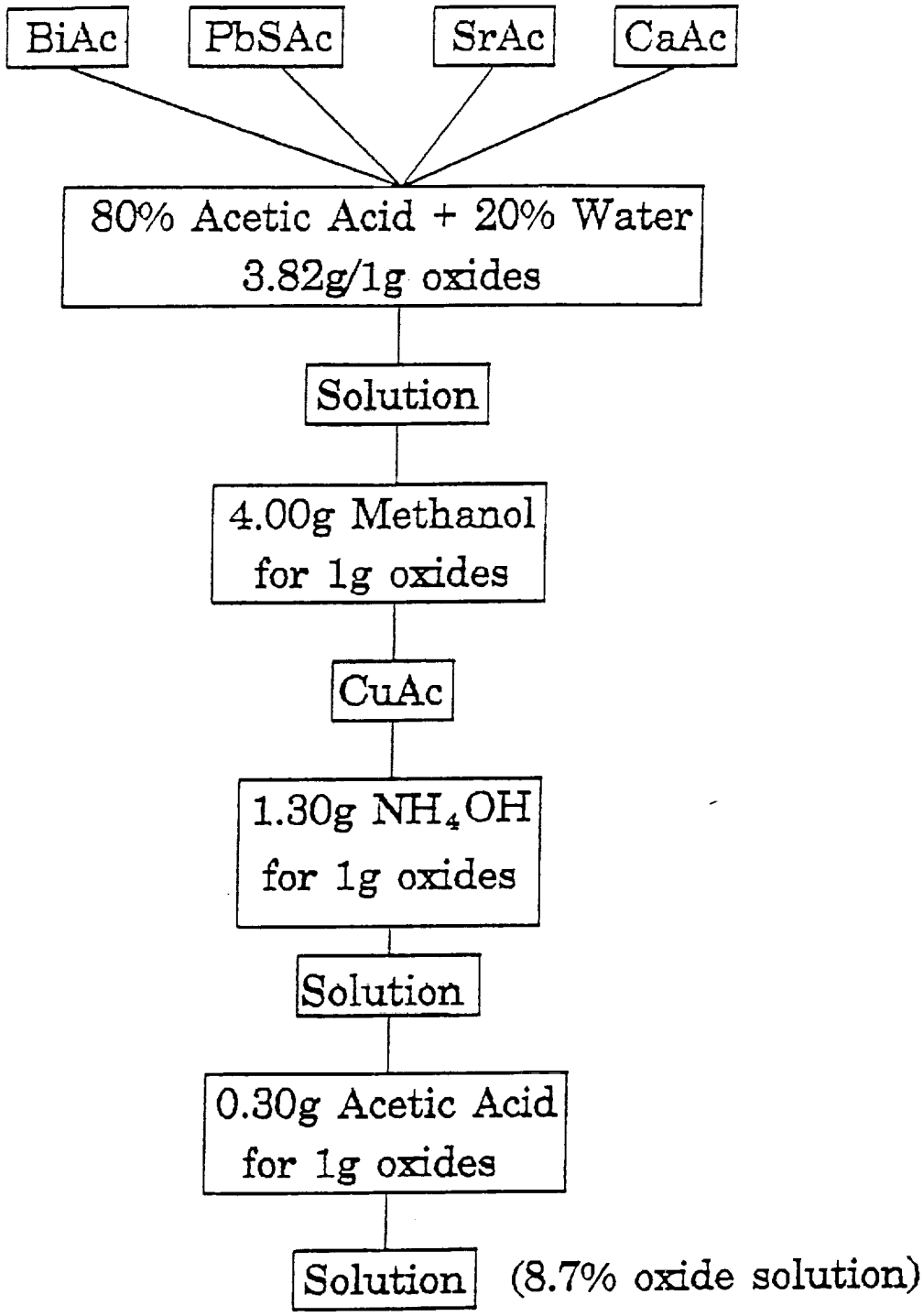

Figure 1 Flow chart for the steps in producing the acetate solution consisting of 8.7% oxides.

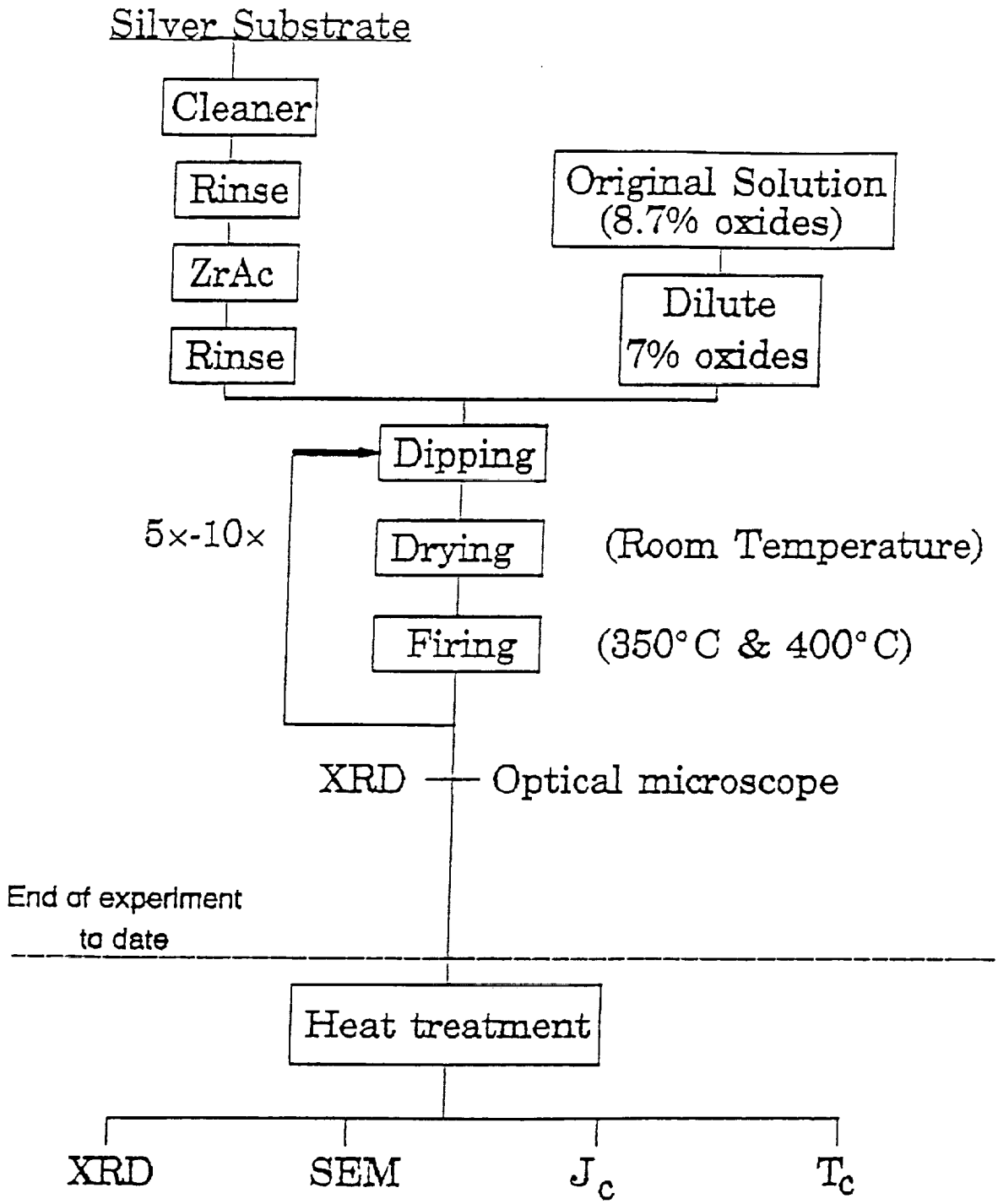

Figure 2 Flow chart of the process for synthesizing superconducting dip coated thin films on silver foil substrates.

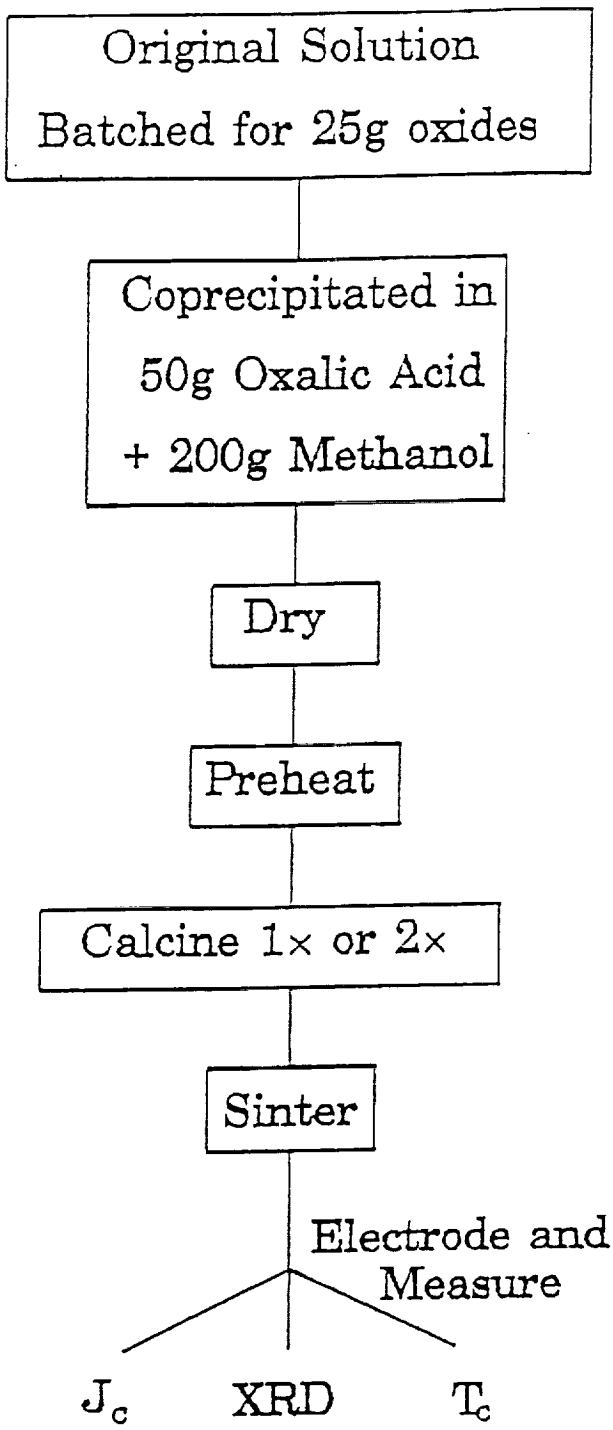

Figure 3 Flow chart for the synthesis of bulk superconducting materials through a coprecipitated powder route.

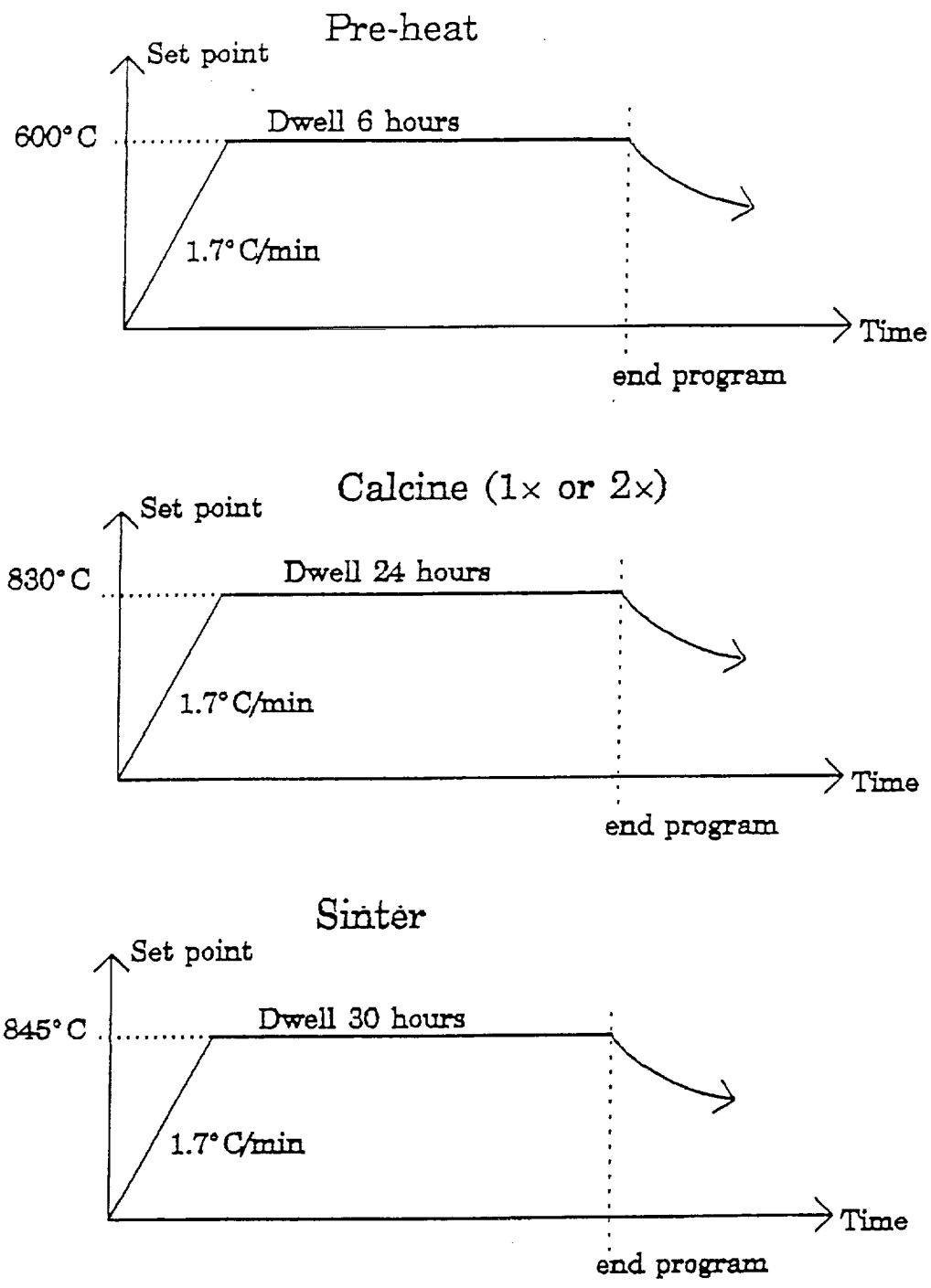

Figure 4 A schematic of the furnace schedules used in pre-heating, calcining, and sintering the bulk material.

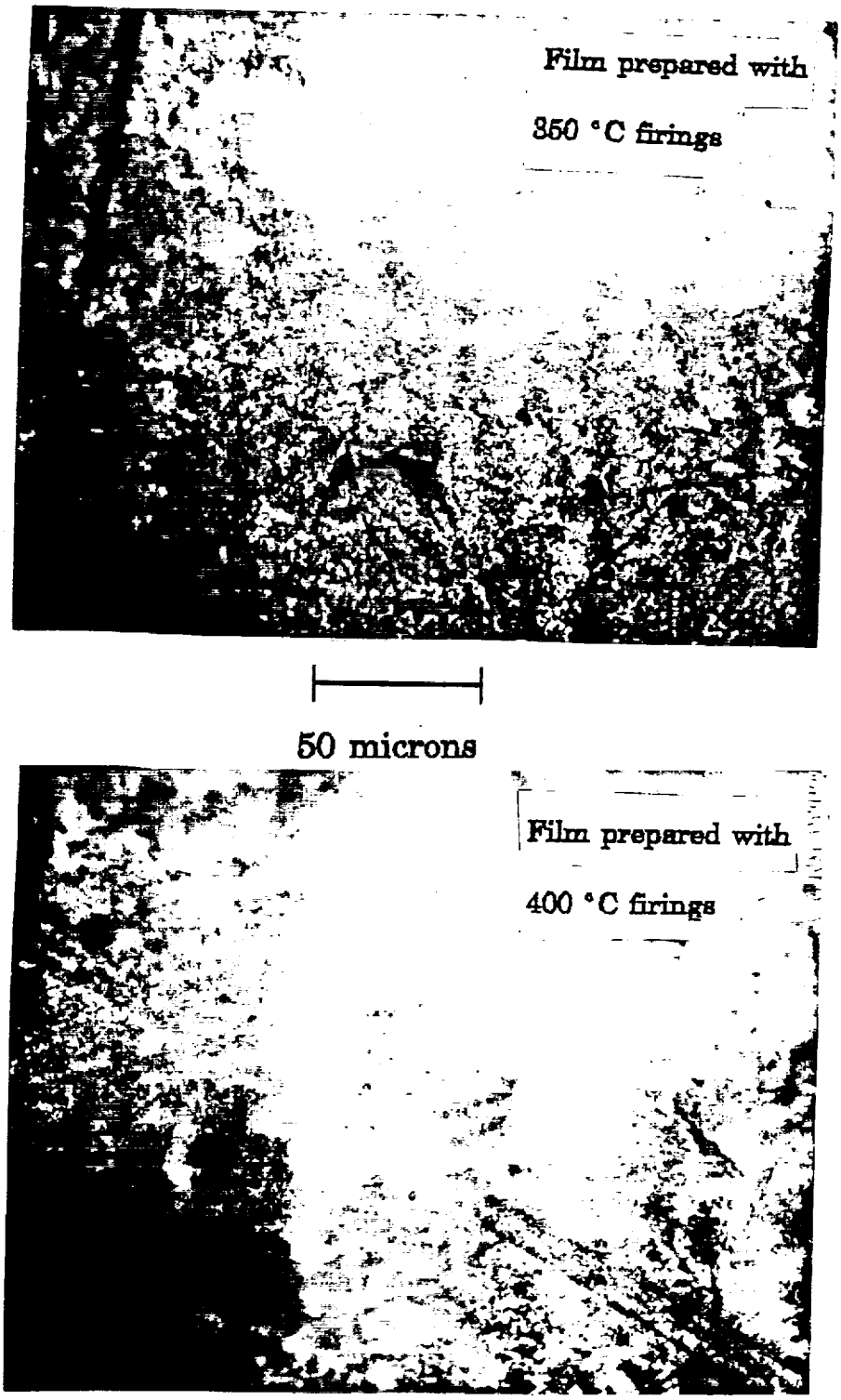

Figure 5 Photomicrographs taken with a Zeiss optical microscope showing the films fabricated on Ag foil with 350°C and 400° firings respectively.

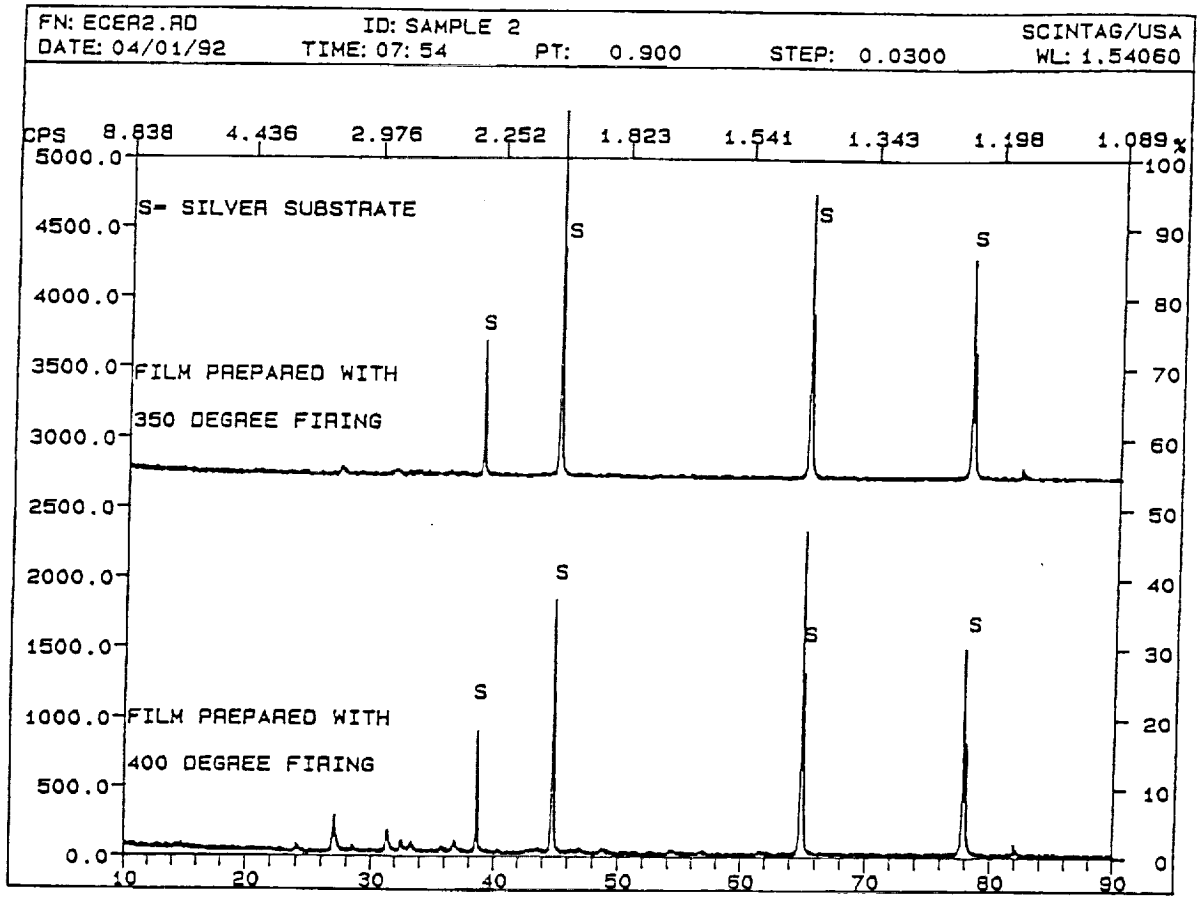

Figure 6 XRD data recorded for the thin films processed with 350 °C and 400 °C firings. Only the peaks from the silver substrate are clearly visible.

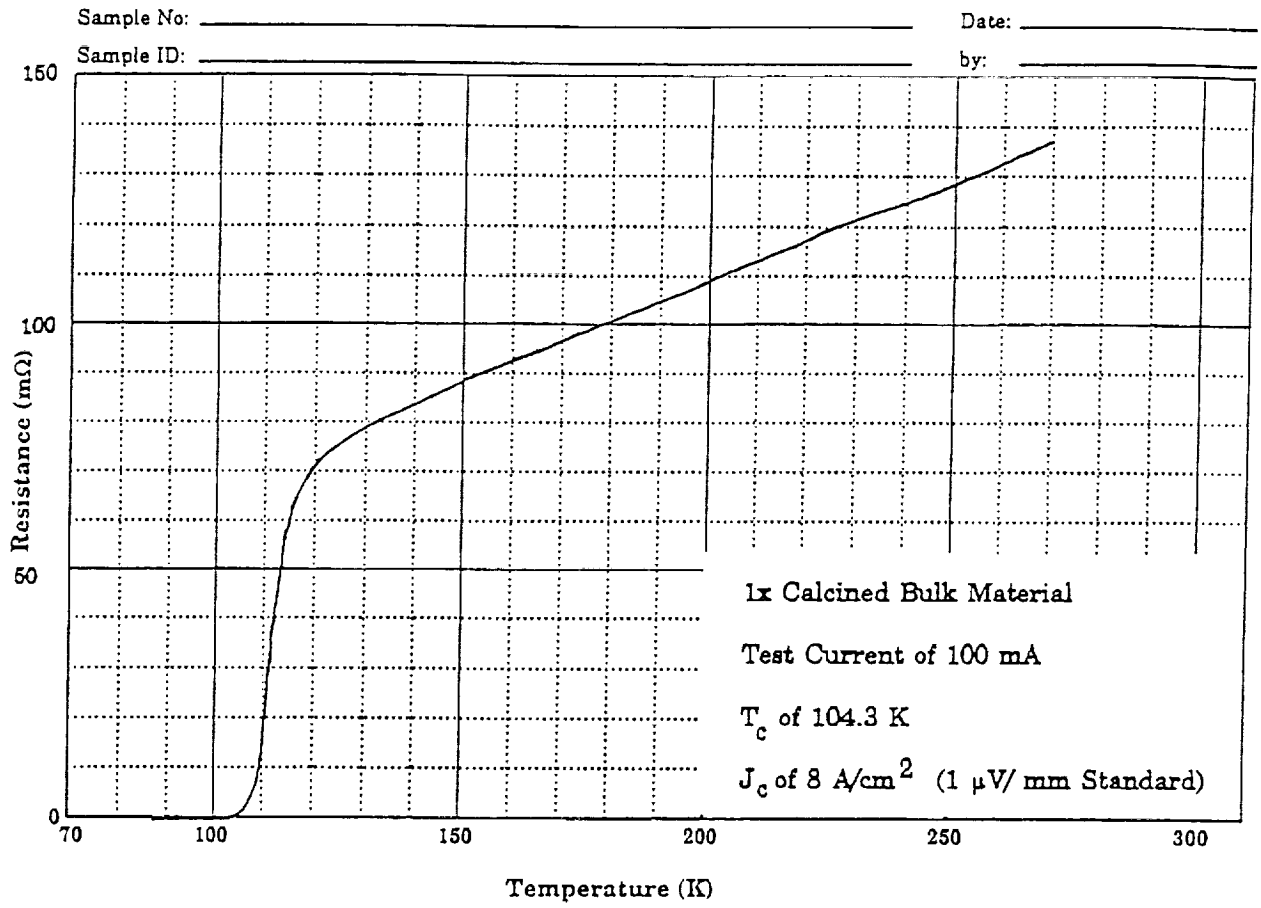

Figure 7 The T_c curve obtained for the bulk material prepared with only one calcine. The figure also shows the relevant testing conditions.

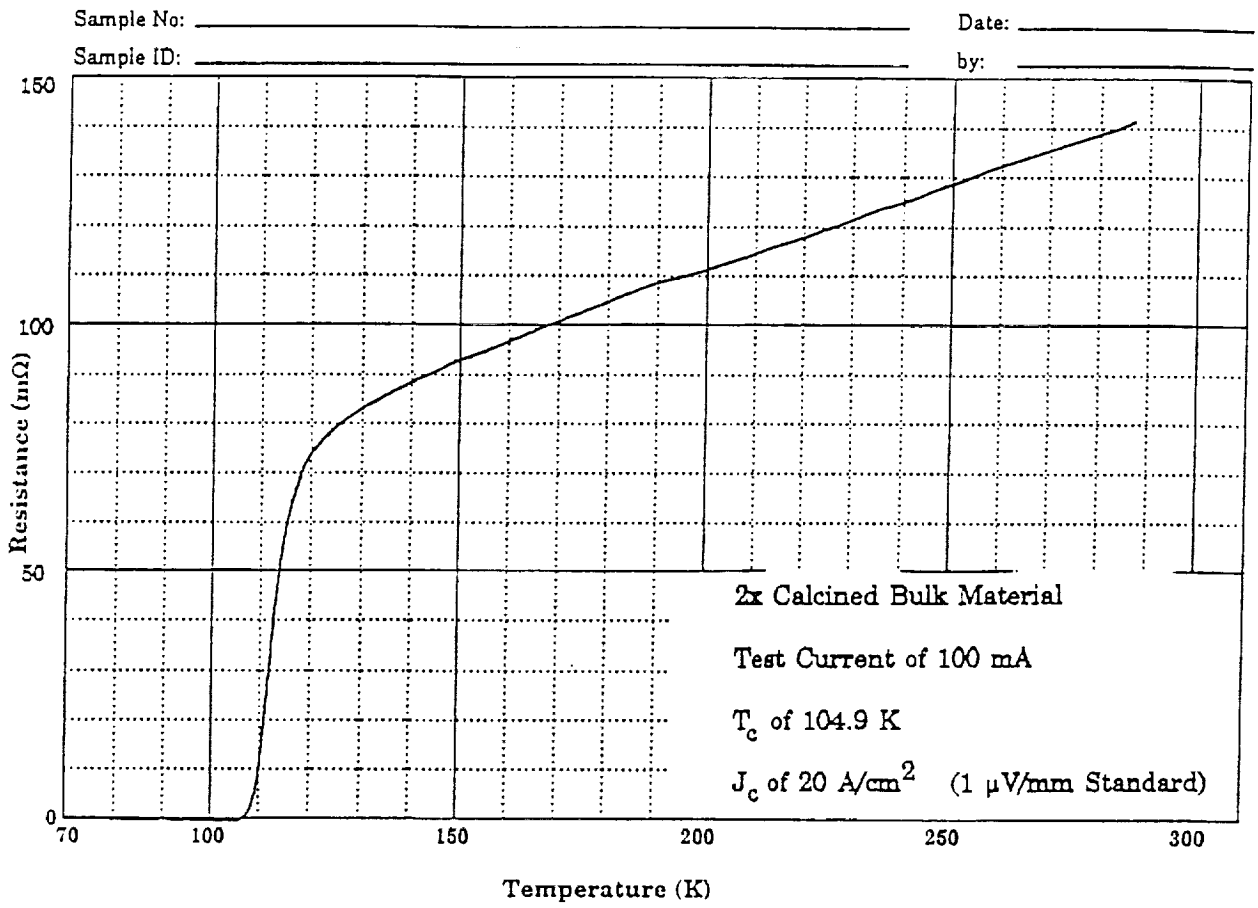

Figure 8 The T_c curve obtained for the bulk material prepared with two calcines. The figure also shows the relevant testing conditions.

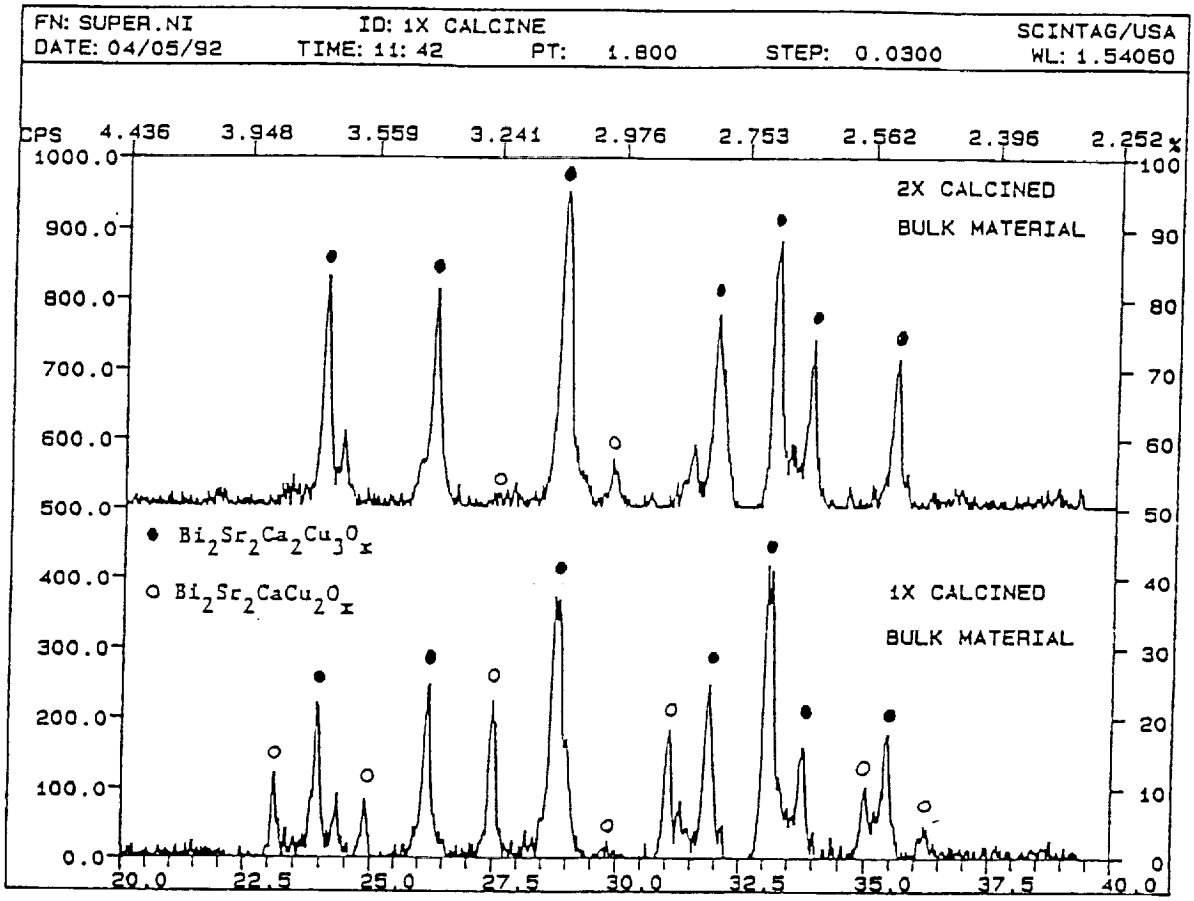

Figure 9 The XRD pattern recorded for the bulk material prepared with one and two calcines. While the once calcined material shows the low and high T_c phases the twice calcined material shows almost pure high T_c phase.

Part III

Semi-Annual Report

SUPERCONDUCTIVITY DEVICES: COMMERCIAL USE OF SPACE

Development of Electrostrictive Ceramic Motor Actuators

to

National Aeronautics and Space Administration
Langley Research Center
Hampton, VA 23665-5225

Principal Investigator:
Gene Haertling -Clemson University

Supporting Investigator:
Guang Li -Clemson University

Contract No. NAG-1-1301

May, 1992

1. Introduction

Electrostriction, which exists in all materials, exhibits many potential applications in electronic and optically controlled systems. Few materials, however, possess electrostrictive effects large enough to be of practical usefulness. The development of materials with high electrostrictive coefficients has been a major impetus of much research in this area. The PBZT ($Pb_xBa_{1-x}(Zr_yTi_{1-y})O_3$) ceramic system appears to be a very promising candidate because the electrostrictive coefficients, Q_{11} and Q_{12}, are among the highest discovered today /1/. In this paper, we describe the preparation and sintering of the PBZT(73/27) ceramic, and the effect of some sintering conditions on sintered samples. The results on the measurement of the electrostrictive and related properties are presented. In addition, a brief discussion of characteristics of PBZT ceramics is provided.

A review of the present state of the technology in ceramic actuators is given in Figure 1. As seen from this figure, a variety of direct motional modes, composite structures and bending modes are employed to produce a given displacement. The maximum displacement per input volt is obtained with composite or bender structures, however, this is usually accomplished at the expense of (1) less load bearing capability, (2) greater complexity, (3) higher cost and (4) lesser reliability. It should be noted that in the simpler direct modes, both piezoelectric and electrostrictive materials are usable; however, the electrostrictors can be driven to higher fields (and hence, higher strains) because they are not limited by ferroelectric domain switching. For example, piezoelectric materials are limited to less than 25 volts/mil (10 kV/cm) due to domain switching which leads to "walk off", but the electrostrictive materials can be used to much higher (50 - 100 volts/mil) fields.

Examples of the strain characteristics of two high strain materials: i.e., PMN:PT and PBZT, are given in Figure 2. Of these, the PBZT materials possess higher intrinsic total strain; and thus, were selected for further investigation and development in this paper.

2. Sample Preparation and Sintering

The PBZT(73/27), $(Pb_{0.73}Ba_{0.27})_{0.97}Bi_{0.02}(Zr_{0.70}Ti_{0.30})O_3$, ceramic samples were prepared and sintered in terms of conventional processing of ferroelectric ceramics. Reagent grade PbO, ZrO_2, TiO_2, $BaCO_3$ and Bi_2O_3 were used as starting raw materials. Weight components were first mixed for two hours, and then calcined at 925°C for two hours. Calcined materials were milled in distilled water using Al_2O_3 balls for 6 hours. Samples were obtained by pressing the ground materials into discs of 12 mm in diameter and about 2 mm in thickness, or plates of 30 x 30 x 5 mm, with water as binder at the pressure of 7000 psi. The samples were sintered at 1250 °C for 4 hours in a closed alumina crucible in an oxygen atmosphere. To avoid the loss of PbO from samples during sintering, a PbO-rich atmosphere was maintained by placing an equalmolar mixture of PbO and ZrO_2 in the crucible. Sintered samples were lapped into different shapes and sizes, depending on the measurement of sample properties. Nickel electrodes were coated onto the opposite sides of samples.

3. Sample Measurements and Results

All the samples exhibited a low-signal dielectric constant of approximately 6400. The resistivities of the samples were sensitive to the sintering conditions; i.e., the oxygen atmosphere, the amount of PbO-ZrO_2 setting powder, sintering temperature, etc.. The relationship between polarization and applied field was measured, as shown in Figure 3. The hysteresis loop indicates that the PBZT(73/27) is a ferroelectric material with a small amount of remanent polarization at room temperature. Several measured parameters of the PBZT(73/27) are illustrated in Table 1.

An experimental device, using an LVDT as a displacement sensor, was made to detect the variation of electrostrictive strains with electric field, which is depicted in Figure 4. Electroded samples were placed in line with the movable cylindrical core of the LVDT which was held in place with a light spring in compression. Care was taken to adjust the spring tension to a proper position to ensure that the measured results are correct. A liquid holder was employed to contain the freon into which samples were immersed so that electric shorting during the application of electric field could be avoided. An electric field was applied to the samples continuously between the negative and positive maxima. The measured results were recorded on a X-Y recorder. The sensitivity of the displacement detection was limited basically by electronic and background vibration noises. The sensitivity of the device was 0.1 μm at a signal-to-noise ratio of 1.

The change of electrostrictive strains, S_1 (longitudinal) and S_2 (lateral), with applied field is illustrated in Figure 5. A small hysteresis corresponding to that of polarization vs. electric field is observed. The electrostrictive hysteresis is estimated to be 5%.

A plot of the strains against square of electric field is shown in Figure 6. It can be seen that the strains vary linearly with the square of electric field at field strengths up to 15 kV/cm. The electrostrictive coefficients, m_{11} and m_{12}, were evaluated from the linear part of the curves, and found to be 4.9×10^{-16} and 2.1×10^{-16} m^2/V^2, respectively. Another form of electrostrictive coefficients, Q_{11} and Q_{12}, relating strain and polarization, were determined by the relationship between the electrostrictive strains and polarization demonstrated in Figure 7. The values obtained are listed in Table 2.

Table 2 also lists electrostrictive coefficients of some commonly used electrostrictive materials for comparison.

4. Discussion

Samples were sintered in oxygen atmosphere in order to increase the density of the sintered samples. Experiment showed that the samples sintered in oxygen environment

have higher translucence, an indication of density, than those without oxygen. Optical microscopic examination also confirmed that the oxygen-sintered samples are more uniform and have less porosity. Another factor, which significantly affects the properties of sintered samples, is the amount of PbO-ZrO_2 setting powder used to maintain a PbO-rich atmosphere around samples during sintering. We found that the optimal amount of setting materials is approximately 20 to 30 weight percent of the samples to be sintered, depending on the shape and size of the samples. Insufficient setting materials result in a dramatic reduction of sample resistivity.

The PBZT(73/27) ceramic may be considered as either Ba-doped PZT or PZT and BZT solid solution since the barium content of the composition is comparable to that of the lead. Pure PZT and BZT solid solution in the same composition used is characterized by a rhombohedral phase at room temperature, as shown in Figure 8 /2/. Additives can transform the characteristic of the rhombohedral phase into relaxor ferroelectric, which is the case we investigated. The relationship between polarization and electric field we obtained exhibits the feature of slim ferroelectric materials. The hysteresis of strains as demonstrated in Figure 5, is undesirable and must be minimized to a reasonable degree before materials are used in practice.

This report gives the initial investigation of the PBZT (73/27) ceramic. Various processing influences can be examined in order to maximize the material performances, such as hot-pressing, varying the composition or additives to reduce strain hysteresis and so on. Furthermore, other features of the system, like temperature characteristics and frequency response, are expected to be evaluated in future work.

5. References

/1/. K. M. Leung, et. al., Ferroelectrics, Vol. 27, pp41 (1980).

/2/. B. Jaffe, Piezoelectric Ceramics, Academic Press (1970)

Table 1

	Dielectric constant	Loss factor	Resistivity (Ohm-cm)	Density (g/cm^3)
PBZT(73/27)	6400	0.10	10^{10}	7.85

Table 2

Electrostrictive Materials	Electrostrictive Coefficients Q_{11} ($x10^3$ m^4/C^2)	Q_{12}	m_{11} ($x10^{16}$ m^2/V^2)	m_{12}	Hysteresis
PMN	15-30	-10	2-5		2%
PZT	20		0.1-0.5		15%
PBZT(73/27)	28	-10	4.9	-2.1	5%

CERAMIC ACTUATOR TECHNOLOGY

Type	Configuration	Load Cap. (lbs.)#	Actuator Movement w/voltage	Actuator Behavior (P or E)*	Actuator Strain (%)**	
					25	100
Monolithic (d_{33} mode)	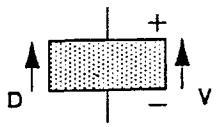	800	Expansion	P	.07	N/A
Monolithic (d_{31} mode)	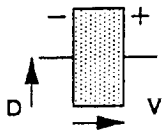	800	Contraction	P	.03	N/A
Monolithic (s_{11} mode)	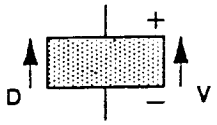	800	Expansion	E	.07	.20
Monolithic (s_{12} mode)	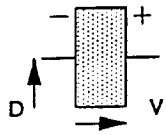	800	Contraction	E	.03	.08
Composite Structure (d_{33} mode) (flexten.)	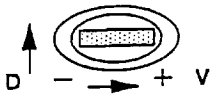	350	Contraction	P	.54	N/A
Composite Structure (d_{33}/d_{31}) (moonie)	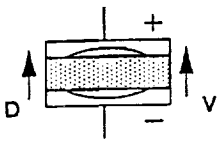	30	Expansion	P	.80	N/A
Monomorph (Bender)	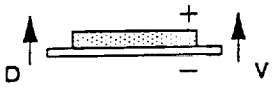	<1	Expansion/ Contraction	P	1.5	N/A
Bimorph (Bender)	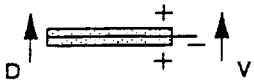	<1	Expansion/ Contraction	P	15.0	N/A

Notes: V = Voltage, D = actuator displacement
\# Maximum load on a 3/4 inch diameter rod
* P = Piezoelectric, E = Electrostrictor
** Strain values at ±25 V/mil (10 kV/cm) & ±100 V/mil (40 kV/cm)

Figure 1.

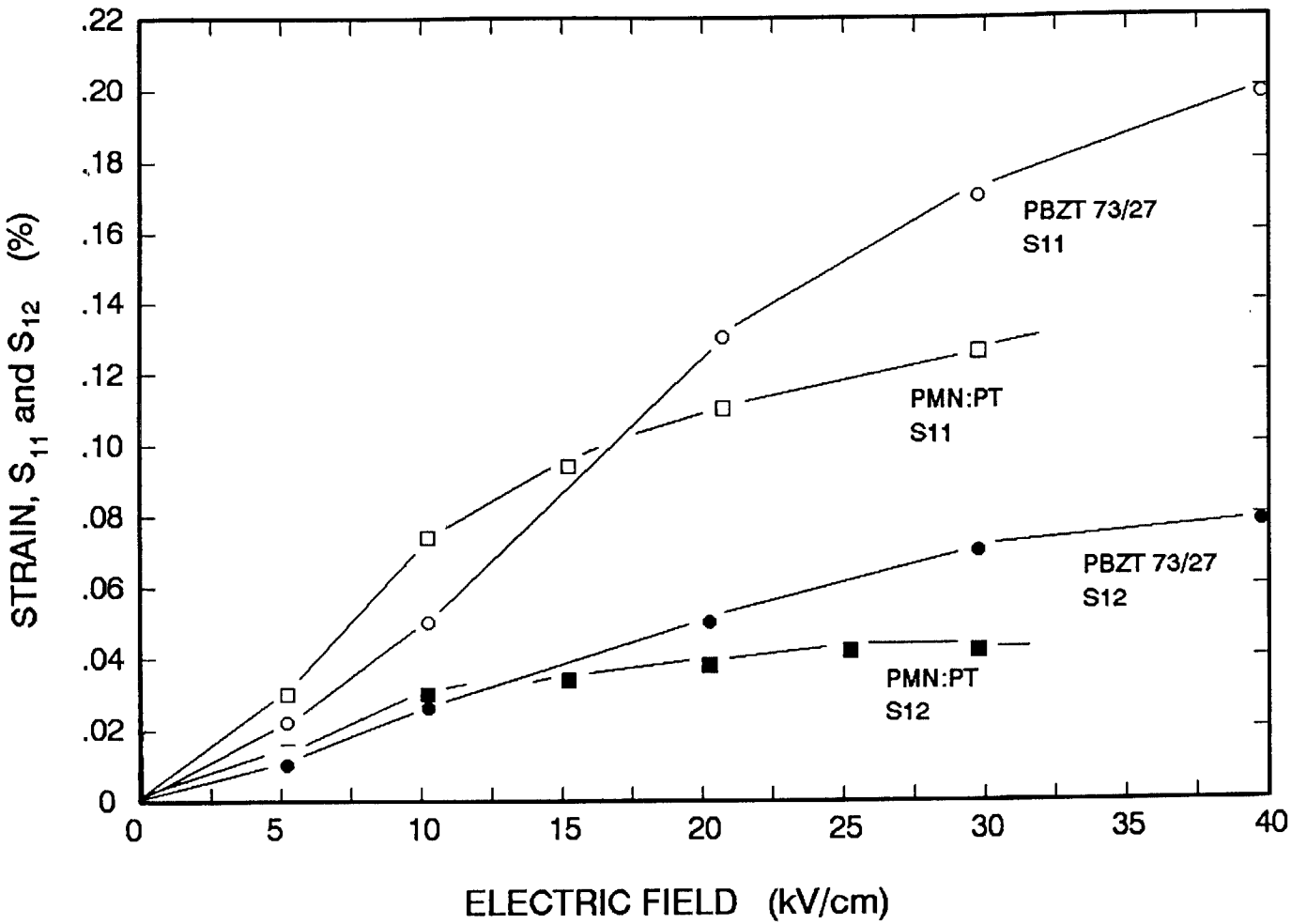

ELECTROMECHANICAL STRAIN BEHAVIOR OF ELECTROSTRICTIVE ACTUATORS .

Figure 2.

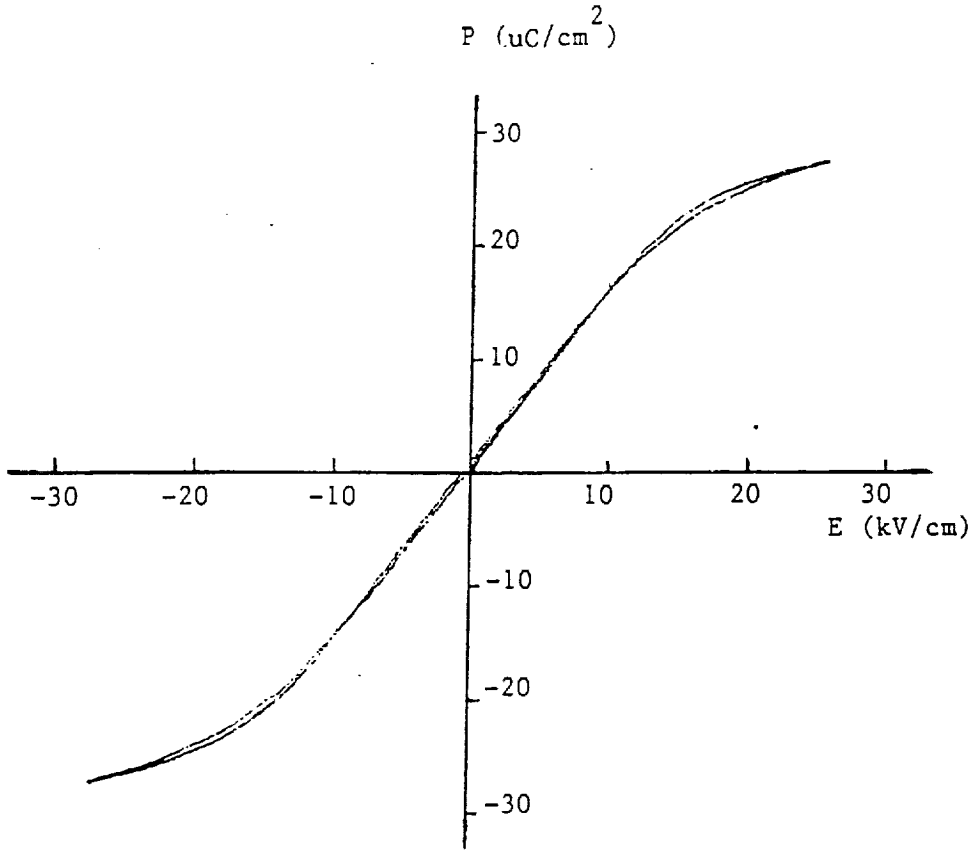

Figure 3. The variationof polarization with electric field for the PBZT (73/27)

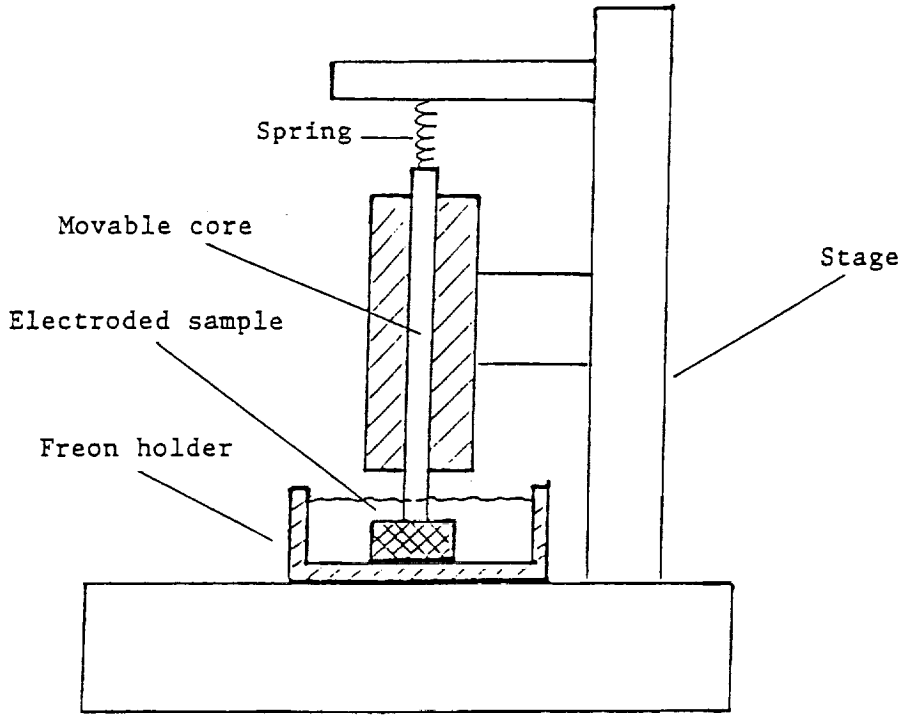

Figure 4. The LVDT device for measurement of electrostriction

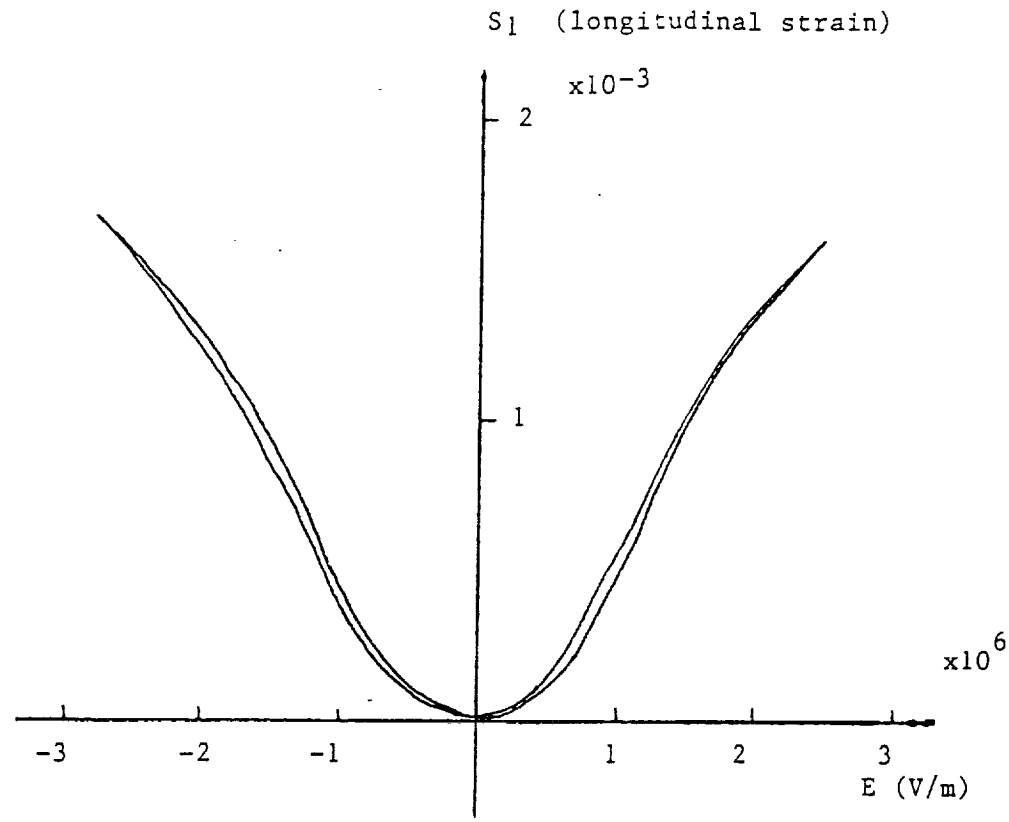

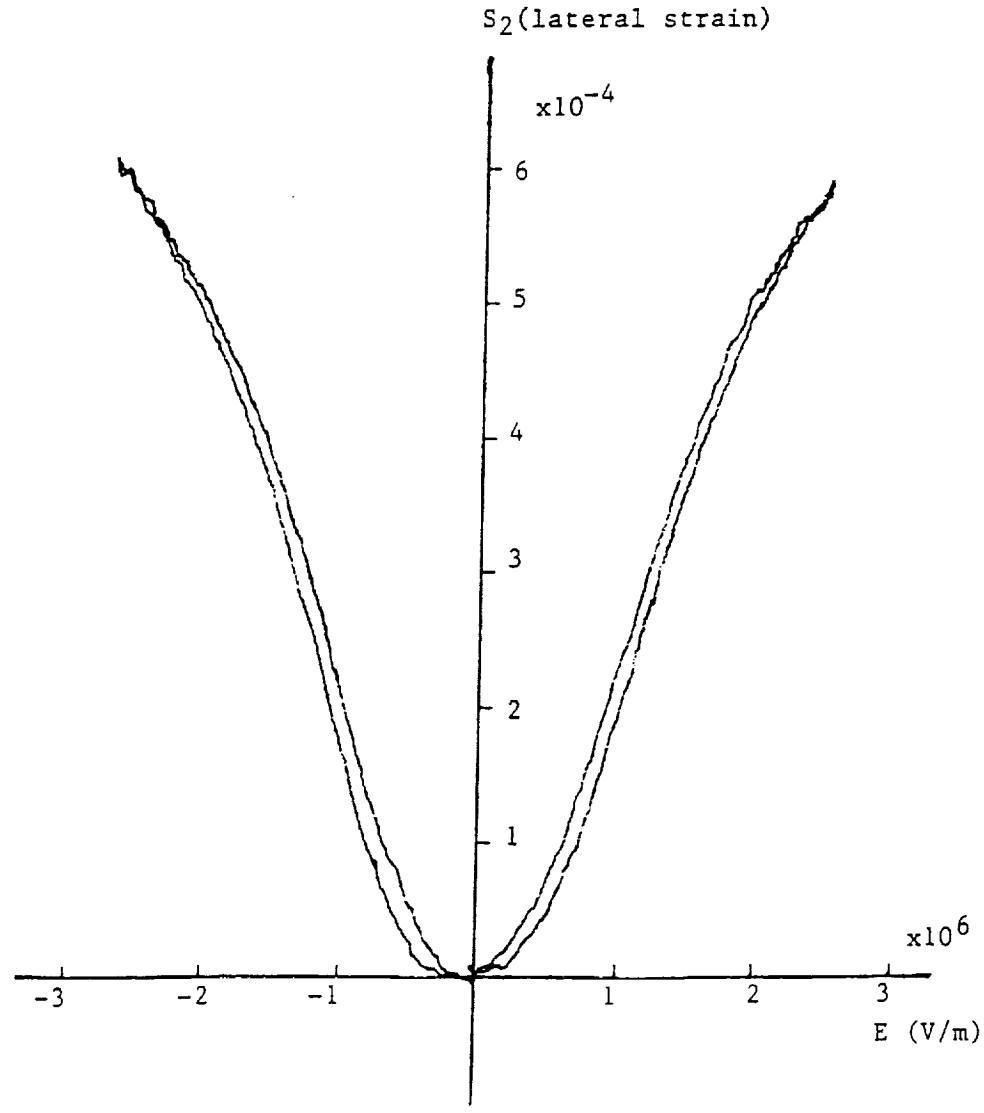

Figure 5. Electrostrictive strains, S_1 and S_2 , vs. electric field

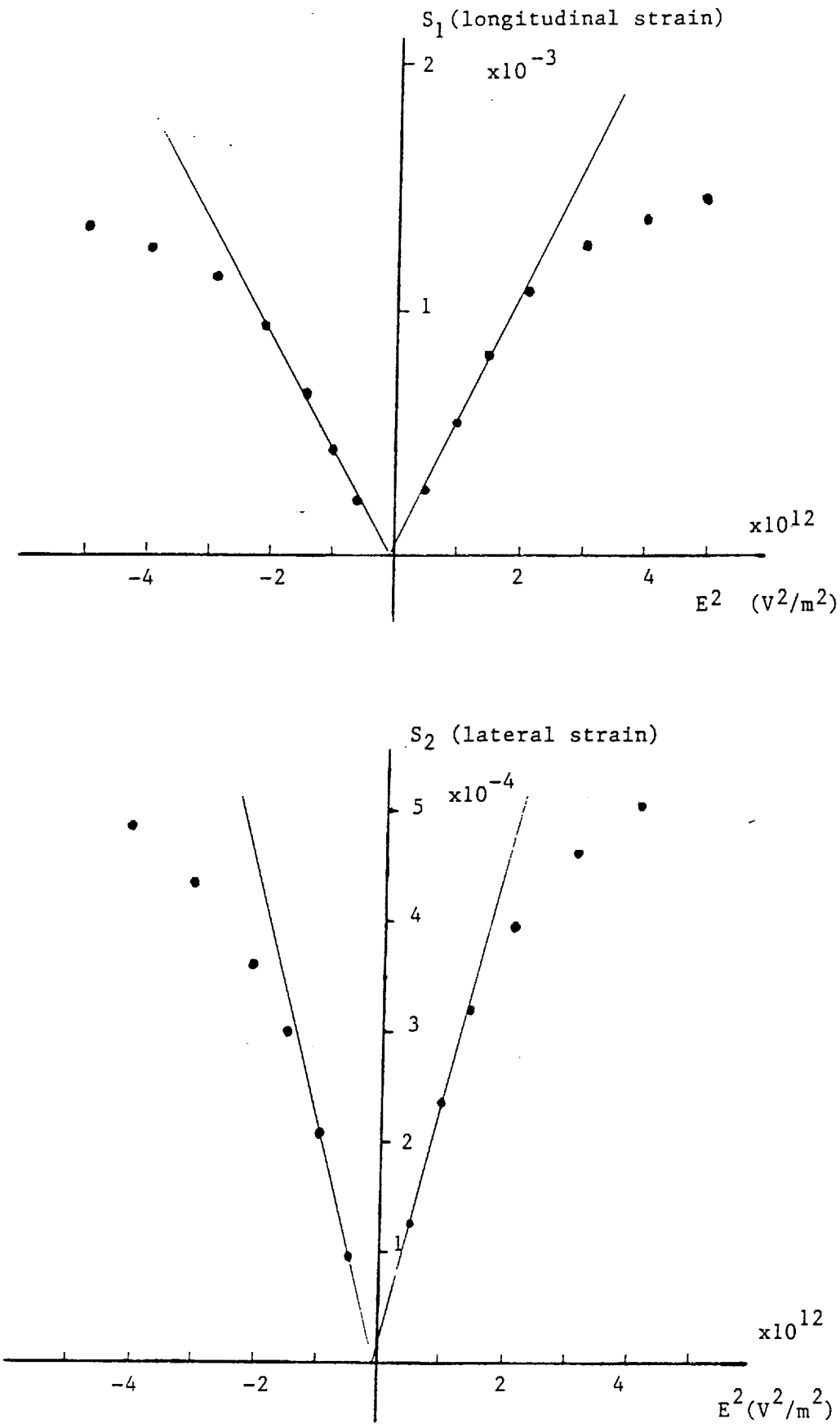

Figure 6. Electrostrictive strains, S_1 and S_2 vs. Square of electric field

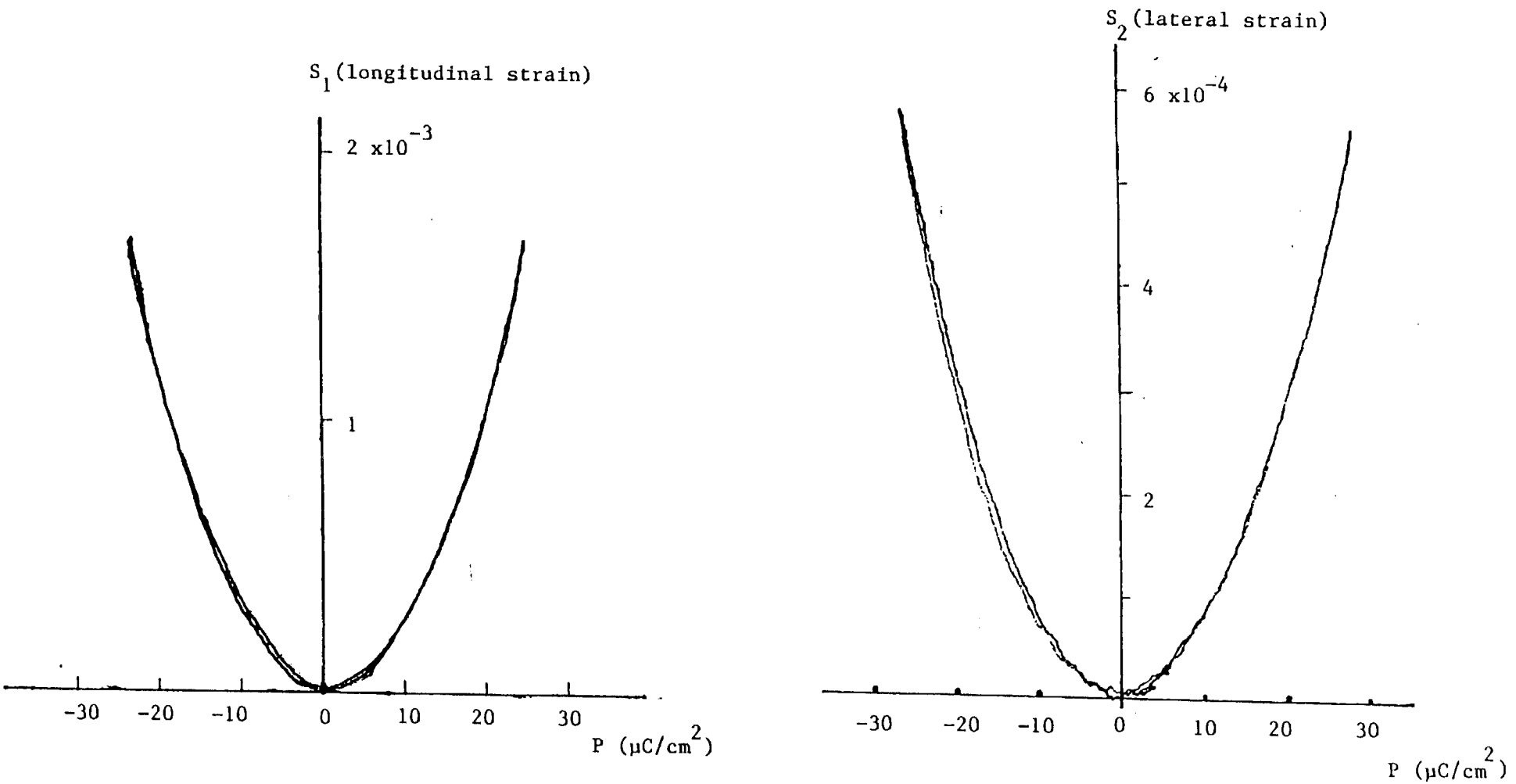

Figure 7. Electrostrictive strains, S_1 and S_2, vs. polarization.

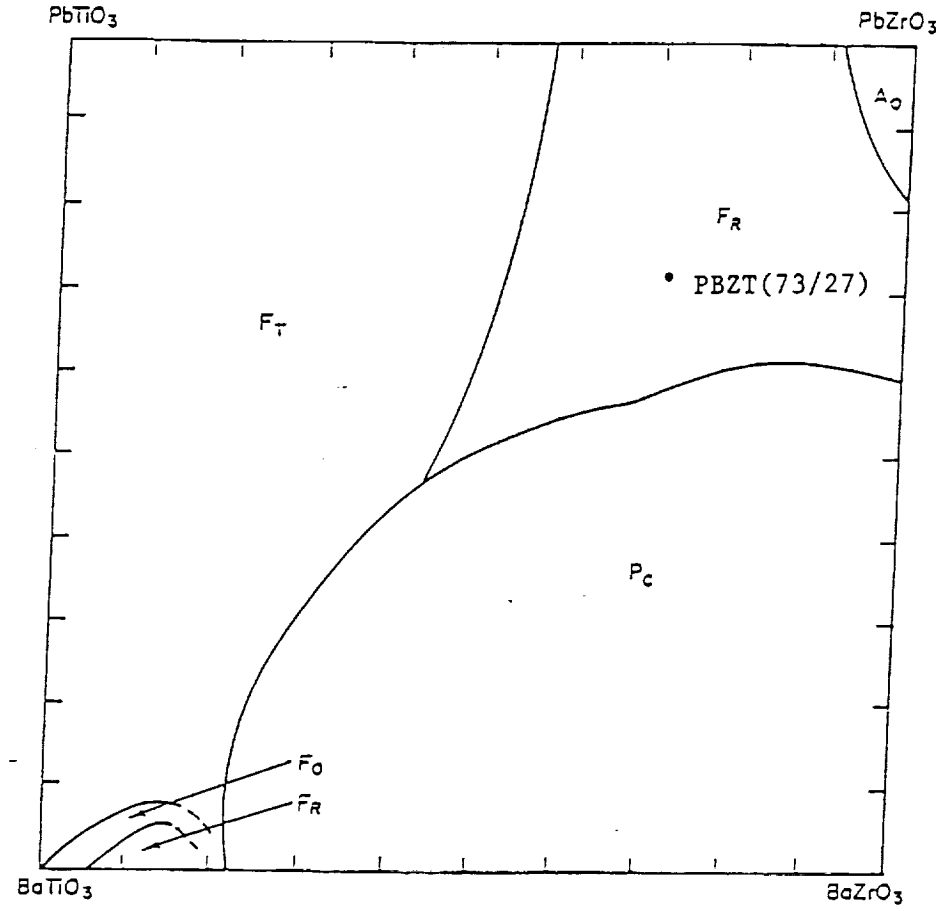

Figure 8. Room temperature phase diagram for system $PbTiO_3$ - $PbZrO_3$ - $BaTiO_3$ - $BaZrO_3$. Fo is orthorhombic BaTiO phase. The PBZT is identified in the figure.